Planetary and Space Science xxx (2017) 1–29

Contents lists available at ScienceDirect

Planetary and Space Science

journal homepage: www.elsevier.com/locate/pss

Massive stereo-based DTM production for Mars on cloud computers

Y. Tao [a,*], J.-P. Muller [a], P. Sidiropoulos [a], Si-Ting Xiong [a], A.R.D. Putri [a], S.H.G. Walter [b], J. Veitch-Michaelis [a], V. Yershov [a]

[a] Imaging Group, Mullard Space Science Laboratory, University College London, Holmbury St Mary, Surrey, RH56NT UK
[b] Planetary Sciences and Remote Sensing Group, Institute of Geological Sciences, Freie Universität Berlin, Germany

ARTICLE INFO

Keywords:
Mars
Global DTM
CTX
HiRISE
CASP-GO
Clouds computing

ABSTRACT

Digital Terrain Model (DTM) creation is essential to improving our understanding of the formation processes of the Martian surface. Although there have been previous demonstrations of open-source or commercial planetary 3D reconstruction software, planetary scientists are still struggling with creating good quality DTMs that meet their science needs, especially when there is a requirement to produce a large number of high quality DTMs using "free" software. In this paper, we describe a new open source system to overcome many of these obstacles by demonstrating results in the context of issues found from experience with several planetary DTM pipelines. We introduce a new fully automated multi-resolution DTM processing chain for NASA Mars Reconnaissance Orbiter (MRO) Context Camera (CTX) and High Resolution Imaging Science Experiment (HiRISE) stereo processing, called the Co-registration Ames Stereo Pipeline (ASP) Gotcha Optimised (CASP-GO), based on the open source NASA ASP. CASP-GO employs tie-point based multi-resolution image co-registration, and Gotcha sub-pixel refinement and densification. CASP-GO pipeline is used to produce planet-wide CTX and HiRISE DTMs that guarantee global geo-referencing compliance with respect to High Resolution Stereo Colour imaging (HRSC), and thence to the Mars Orbiter Laser Altimeter (MOLA); providing refined stereo matching completeness and accuracy. All software and good quality products introduced in this paper are being made open-source to the planetary science community through collaboration with NASA Ames, United States Geological Survey (USGS) and the Jet Propulsion Laboratory (JPL), Advanced Multi-Mission Operations System (AMMOS) Planetary Data System (PDS) Pipeline Service (APPS-PDS4), as well as browseable and visualisable through the iMars web based Geographic Information System (webGIS) system.

1. Introduction

1.1. Background and context

Almost fifty-two years have elapsed since the first pictures of the Martian surface were taken by the NASA Mariner 4 spacecraft. Over that time, the resolution and quality of orbital imagery has improved from tens of kilometres down to 25 cm. During these 5 decades, many areas on Mars have been imaged with serendipitous stereo, mainly to improve the potential for scientific studies. The rapid progress in planetary surface reconnaissance instrumentation, especially in relation to 3D imaging of the surface, has allowed change detection analysis. For example, by overlaying different high-resolution (<100m/pixel) imagery from distinct time epochs (starting back to the mid 1970's) one can examine dynamic features, such as the recent discovery on Mars of mass (e.g. boulder) movement, tracking inter-year changes of seasonal phenomena (e.g. Swiss Cheese Terrain) and looking for fresh craters from meteoritic impacts.

It is common knowledge in the planetary scientific community that research greatly benefits from the availability of high-resolution 3D models of Mars. Even though over the last 20 years there has been substantial progress in the development of either open-source or commercial planetary 3D reconstruction software, such software typically fails to reach the required performance when used by individual planetary scientists to build good quality Digital Terrain Models (DTMs) on their own.

Within the recently completed European Union's Seventh Framework Programme (EU FP-7) iMars (http://www.i-mars.eu last accessed: 15.11.2017) project, we focused on developing tools and producing

* Corresponding author.
E-mail addresses: yu.tao@ucl.ac.uk (Y. Tao), j.muller@ucl.ac.uk (J.-P. Muller), p.sidiropoulos@ucl.ac.uk (P. Sidiropoulos), siting.xiong.14@ucl.ac.uk (S.-T. Xiong), alfiah.putri.15@ucl.ac.uk (A.R.D. Putri), sebastian.walter@fu-berlin.de (S.H.G. Walter), j.veitchmichaelis.12@ucl.ac.uk (J. Veitch-Michaelis), v.yershov@ucl.ac.uk (V. Yershov).

https://doi.org/10.1016/j.pss.2018.02.012
Received 5 September 2017; Received in revised form 10 January 2018; Accepted 16 February 2018
Available online xxxx

value-added datasets to maximize the exploitation of the available planetary datasets of the Martian surface. This includes the generation of high quality co-registered DTMs and corresponding terrain-corrected OrthoRectified Images (ORIs), using data from different NASA and ESA instruments.

In this paper, we introduce a fully automated multi-resolution DTM processing chain developed by the Imaging Group at Mullard Space Science Laboratory (MSSL) at University College London (UCL) for NASA Mars Reconnaissance Orbiter (MRO) Context Camera (CTX) and High Resolution Imaging Science Experiment (HiRISE) stereo-pairs. This is called the Co-registration Ames Stereo Pipeline-Gotcha Optimised (CASP-GO). This pipeline is based on the open source NASA Ames Stereo Pipeline (ASP) (Becker et al., 2013; Moratto et al., 2010; Shean et al., 2016), the UCL Automated Co-registration and Ortho-rectification (ACRO) pipeline (Sidiropoulos and Muller, 2015; Sidiropoulos and Muller, 2017), and the Gotcha (Shin and Muller, 2012) sub-pixel refinement method. The implemented system guarantees global geo-referencing compliance with respect to the ESA Mars Express High Resolution Camera (HRSC), and hence to the Mars Orbiter Laser Altimeter (MOLA), providing refined stereo matching completeness and accuracy from the open-source ASP normalised cross-correlation implementation.

We have created a set of complete and fused 3D models (~5500 CTX and ~400 HiRISE stereo products) of the Martian surface from multi-resolution co-registered stereo that are all co-registered to a global reference system derived from laser altimetry. This allows a much more comprehensive interpretation based upon a multi-resolution analysis of the Martian surface to be made. A large sample of the DTM product was randomly selected for quality validation by visual inspection. The processed DTMs are integrated into a developed web based Geographic Information System (webGIS) which allows experts and members of the public to examine different parts of the planet for changes as well as to perform geomorphological and geological research.

In the near future, it is planned to release the CASP-GO system as open-source, once we have included the latest ESA ExoMars Trace Gas Orbiter (TGO) Colour and Stereo Surface Imaging System (CaSSIS) data. Potentially, the iMars base data can also be used by the TGO mission and subsequent ESA missions to provide the necessary inputs for selection of a future landing site such as the ESA ExoMars 2020 rover and for any Mars Sample Return missions in the 2020s. In the iMars webGIS, we have all the NASA rover sites and planned ExoMars rover landing sites available in a full range of 3D HRSC, CTX and HiRISE DTMs and terrain-corrected images. The NASA rover sites, in addition, have a gateway to a separate webGIS containing processed rover camera data. In all cases, a 3D digitisation tool called PRo3D® (Traxler et al., 2017) developed within a previous EU-FP7 Planetary Robotics Vision Data Exploitation (PRoViDE) project (http://provide-space.eu last accessed: 15.11.2017) is available through the webGIS system.

We discuss issues arising from experimenting with well-known open-source and commercial planetary DTM software in comparison with several in-house DTM processing pipelines. We comment, particularly on the use of the open-source ASP DTM processing chain and introduce a new working solution based on ASP. These issues include global co-registration accuracy, de-noising, dealing with match failure, matching confidence estimation, outlier detection and discarding scheme, various DTM artefacts, uncertainty estimation, and quality-efficiency trade-offs. Examples of DTM processing results from CTX over the United States Geological Survey (USGS) MC11 map quadrant area (bounded by latitudes 0°, 30°N and longitudes 315°, 360°E) are provided. Internal comparison and evaluation between different DTM pipelines are also here shown for the Mars Exploration Rover (MER) and Mars Science Laboratory (MSL) landing sites.

The rest of the paper is structured as follows. In the next subsection 1.2, we review the datasets employed followed in section 2 by an inter-comparison of different DTM processing pipelines and in section 3, the CASP-GO system that has been developed. In section 4, examples of different CTX DTM and ORI products are presented as well as the development of a planet-wide CTX processing system. In section 5, issues concerned with data formats, dissemination and the relationship of CASP-GO to ACRO is explained. Finally, in section 6, we discuss the overall results and provide pointers to future developments.

1.2. Dataset overview

The fundamental global reference system is based on MOLA data for our multi-resolution DTM production. MOLA is considered to be the most accurate and internally consistent global Mars 3D reference model developed to date. Individual MOLA tracks were interpolated and extrapolated by the MOLA team (Smith et al., 2001) to yield a global MOLA DTM with a spatial resolution of up to 128 grid-points per degree (463m) and a vertical track-crossing difference of between 2 and 13m. For the polar regions, an interpolated MOLA DTM is available with a spatial resolution of 512 grid-points per degree (108m). These MOLA DTMs are available through the NASA Planetary Database System (PDS; http://pds-geosciences.wustl.edu/missions/mgs/megdr.html last accessed: 15.11.2017).

The HRSC on Mars Express comprises nine channels/looks that together in a single pass, within a few minutes, collect multi-angular and multi-colour images of the Martian surface, allowing stereo colour images to be produced from single orbit observations (Gwinner et al., 2016). German Aerospace Centre (DLR) has generated along-track orbital strip DTMs (at grid-spacing from 50-150m) and ORIs (up to 12.5m/pixel) in a Sinusoidal projection system. The processing of the raw HRSC data includes radiometric de-calibration, noise reduction, image matching, geo-referencing, photogrammetric processing and along-track Bundle Adjustment (BA). The final products are then labelled as "Level-4 Version 50+" (v50+) when the products reach a satisfactory level of quality (Gwinner et al., 2009; Gwinner et al., 2016). The co-registration of HRSC DTM and MOLA DTM is checked using average height differences and usually reveal residual horizontal offsets smaller than the grid spacing of the HRSC DTM and residual vertical offsets below 10m (Gwinner et al., 2009).

The v50 + HRSC DTMs use the MOLA reference sphere with a radius of 3396.0 km. In iMars, the v50 + HRSC ORI/DTMs have been employed for most of the initial sites as a reference base map, so that the CTX products can be co-registered with HRSC and CTX 3D mapping products can subsequently be employed as the baseline for auto-co-registration and orthorectification for higher resolution images such as Mars Observer Camera Narrow-Angle (MOC-NA) and HiRISE. Almost all of the Martian surface has been covered by HRSC data but only around half has been processed into corresponding DTMs and ORIs.

More recently, with increasingly dense HRSC level-4 coverage, a large-area mosaic has been generated by DLR/Leibniz University of Hanover (LUH)/Free University of Berlin (FUB) over the USGS MC11 map quadrangle (MC11-E: 0 to 62.5 km in the north and east directions from the origin; MC11-W: 0 to 62.5 km in the north and west directions from the origin) (Gwinner et al., 2015). This quadrant includes three of the four proposed ExoMars 2018 landing site candidates. The MC11 HRSC DTM mosaic uses Equidistant Cylindrical projection with a grid spacing of 50m for the DTM and colour mosaics, and 12.5m for the panchromatic image mosaic. The MC11 mosaicked DTM and ORI are based on the same set of procedures for image filtering and rectification, least squares matching, strip Bundle Adjustment, and calculation of 3D points applied for single strip data products. In addition, a bundle block adjustment, joint interpolation of multi-scale 3D point data sets, and photometric correction and image normalisation with respect to an external brightness standard (Thermal Emission Spectrometer albedo) are applied for the ORI mosaic (Gwinner et al., 2016).

HRSC provides the fundamental 3D mapping products used here for the baseline, where they are available (i.e. for approximately 50% of Mars). When CTX stereo products are also available over the same areas as HRSC (i.e. for approximately 20% of the surface) then the CTX

products can be co-registered with HRSC and CTX 3D mapping products can be employed as the baseline for 3D rectification of higher resolution images such as MOC-NA and HiRISE.

In parallel since 2007, the MRO CTX instrument captures repeat pass single panchromatic grey-scale images at ~6m/pixel over a swath-width of 30km with a large number with suitable stereo angles (Cook et al., 1996).

The current work builds upon experience that was gained when we initially processed CTX stereo pairs for the MER-A (Spirit), MER-B (Opportunity), MSL, Viking-1, Viking-2, Mars Pathfinder (MPF), and Phoenix to derive ORIs (6m) and DTMs of 18m/grid point resolution using the ASP software in early 2013 within the EU-FP7 PRoViDE project. CTX ORI and DTMs are essential for accurate HiRISE to HRSC co-registration. In late 2015, within the iMars project, CTX stereo pairs for MER-A, MER-B, and MSL were reprocessed at UCL using the optimised CASP-GO processing chain, which brings CTX ORI and DTM to a higher level of quality compared to the ASP based results produced in the PRoViDE project. Moving towards global processing of CTX stereo pairs, more recently, a total of ~5500 planet-wide CTX stereo pairs have been processed by UCL using the CASP-GO system ported to the Microsoft® Azure® computing cloud. These results will be described in more detail in section 5.

Finally, the NASA MRO HiRISE camera is designed to acquire very detailed orbital images of Mars at resolutions up to 25cm. HiRISE uses 14 Charged Coupled Device (CCD) pushbrooms in a Time Delay Integration (TDI) including 10 red channels, 2 blue-green channels, and 2 Near-infrared (NIR) channels. The nominal maximum size of the red images is about 20,000 × 126,000 pixels and 4000 × 126,000 pixels for the narrower Blue-Green (B-G) and NIR bands. To facilitate the mapping of landing sites, HiRISE produces stereo pairs of images from which the topography can be measured to a precision of 0.25 metres. The HiRISE images are usually acquired at the same time as CTX (Malin & McEwen, private communications, 2015, 2016). At the time of writing, 441 HiRISE stereo pairs have been identified for processing. These pairs were prioritised because they belong to areas that have 5 or more repeat views.

2. Related work

2.1. An overview of planetary DTM processing pipelines

DTM creation is essential to improve our understanding of the geology and geomorphology of the Martian surface. Although there have been demonstrations of different open-source or commercial planetary 3D reconstruction software, geologists are still struggling to create good quality DTMs that meet the needs of their scientific application, especially when there is a need to produce a large number of high quality DTMs using "free" software.

Generally speaking, different DTMs from different pipelines display different kinds of artefacts. For example, the Ohio State University (OSU) HiRISE DTM employed within the PRoViDE project (Li et al., 2008) has mis-matched outliers in some crater regions, the ASP processing chain displays a quilting artefact caused by use of an initial integer based cross-correlation, matching gaps for texture-less places from multiple DTM pipelines, and there are known artefacts in the University of Arizona (UoA)/USGS products, such as "Boxes", CCD seams, faceted areas and manually interpolated areas (see https://hirise.lpl.arizona.edu/dtm/about.php for more details; last accessed 15.11.2017).

These artefacts are typically considered minor issues for Geographic Information System (GIS) and visualisation after a down-sampling of DTM spacing of 3:1 from full resolution. However, for a detailed geological study of selected sites, a DTM at a higher level of quality and lower level of artefacts is desirable.

Before developing our own DTM production pipeline, within iMars, we initially investigated several planetary DTM pipelines, taking advantage particularly of open source systems, and further extended/modified several key components to specifically address issues found from the experimental products, in order to improve the performance of the processing chain. The different DTM pipelines that were examined are presented and discussed in the following sub-sections.

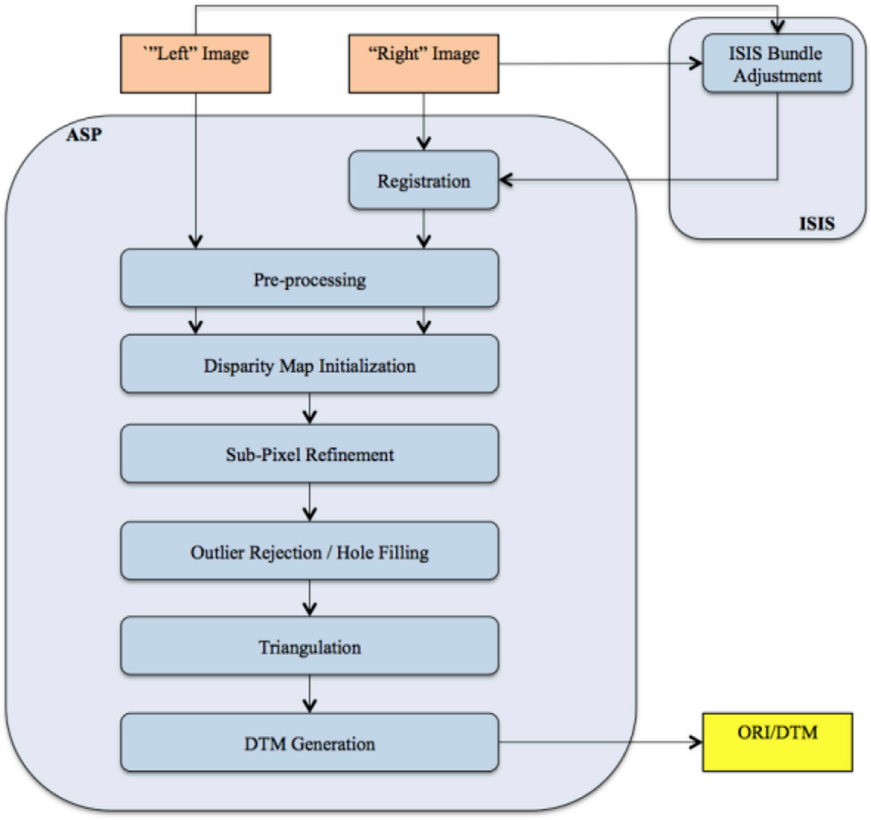

Fig. 1. Flow diagram of the original ASP processing chain described in (Becker et al., 2013).

2.2. NASA Ames Stereo Pipeline

The original ASP software was developed by the Intelligent Robotics Group (IRG) of Intelligent Systems Division at the NASA Ames Research Centre (Moratto et al., 2010). ASP is a suite of automated geodesy and stereo-photogrammetry tools designed for processing planetary imagery captured either from planetary (robotic) orbiters and landers or from Earth satellites. It was designed to process stereo imagery captured by NASA and commercial spacecraft and produce cartographic products including DTM, ORI, and 3D point cloud models. It is built on the Vision Workbench software (https://github.com/visionworkbench/visionworkbench/wiki last accessed: 10.01.2018), which is a general-purpose image processing and computer vision library integrated into the USGS Integrated Software for Imagers and Spectrometers (ISIS) (Becker et al., 2013; Beyer, 2015; Edwards, 1987).

(Fig. 1) shows a schematic flowchart of the key processes involved in the ASP DTM pipeline. ASP takes ISIS (which can be distinguished by their ".cub" suffix) "left" and "right" images as input and starts stereo processing. The processing stages are as follows: (a) pre-processing, including least squares BA, left-right image alignment, map projection that eliminates some of the perspective differences leaving only small perspective differences in the images, image normalisation to bring the two images into the same dynamic range, and image filtering to reduce noise and extract edges; (b) disparity map initialisation that uses a pyramid tiled, integer based correlation approach to find fast correspondences between pixels in the left and right images; (c) sub-pixel refinement to obtain sub-pixel correlation from their integer estimates; (d) triangulation that uses the geometric camera models stored in ISIS cub files to find the closest point of "intersection" of the two camera rays from disparity map and finally (e) DTM and ORI generation.

The original ASP pipeline was investigated in the early stages of the iMars project. A quality assessment of the processed results was made by comparing the output DTMs with those produced from the BAE SOCET® system, the University of Seoul (UoS) pipeline (Kim and Muller, 2009) and the École Polytechnique Fédérale de Lausanne (EPFL) pipeline (Ivanov and Lorre, 2002; Ivanov, 2003) applied to the same regions on Mars. For this purpose, input CTX and HiRISE stereo images of the three most observed sites on MER and MSL were chosen. The supporting (reference) DTMs and images were taken from the HRSC products overlapping with the CTX images.

2.3. BAE SOCET® system

The USGS-ISIS software can also be used together with the Soft Copy Exploitation Tool Set, called BAE SOCET® Set (SS) (http://www.baesystems.com; http://webgis.wr.usgs.gov/pigwad/tutorials/socetset/SocetSet4HiRISE.htm last accessed: 15.11.2017), for creating DTMs. The flow chart of this process is shown in (Fig. 2). USGS-ISIS is used to reformat the level-0 input into level-1 radiometrically corrected images which are then ingested into SS for bundle adjustment and stereo matching as well as grid-point interpolated onto a regular DTM and ORI as before. See (Kirk et al., 2008) for further details of this USGS processing system based on ISIS and SS.

The ISIS processing system includes ingestion of the input experimental data record (EDR) images, radiometric and geometric correction of the images (creating undistorted images based on an idealised camera model), creating a ground-control network and then processing them in the SS workstation, which uses the automatic terrain extraction (ATE;

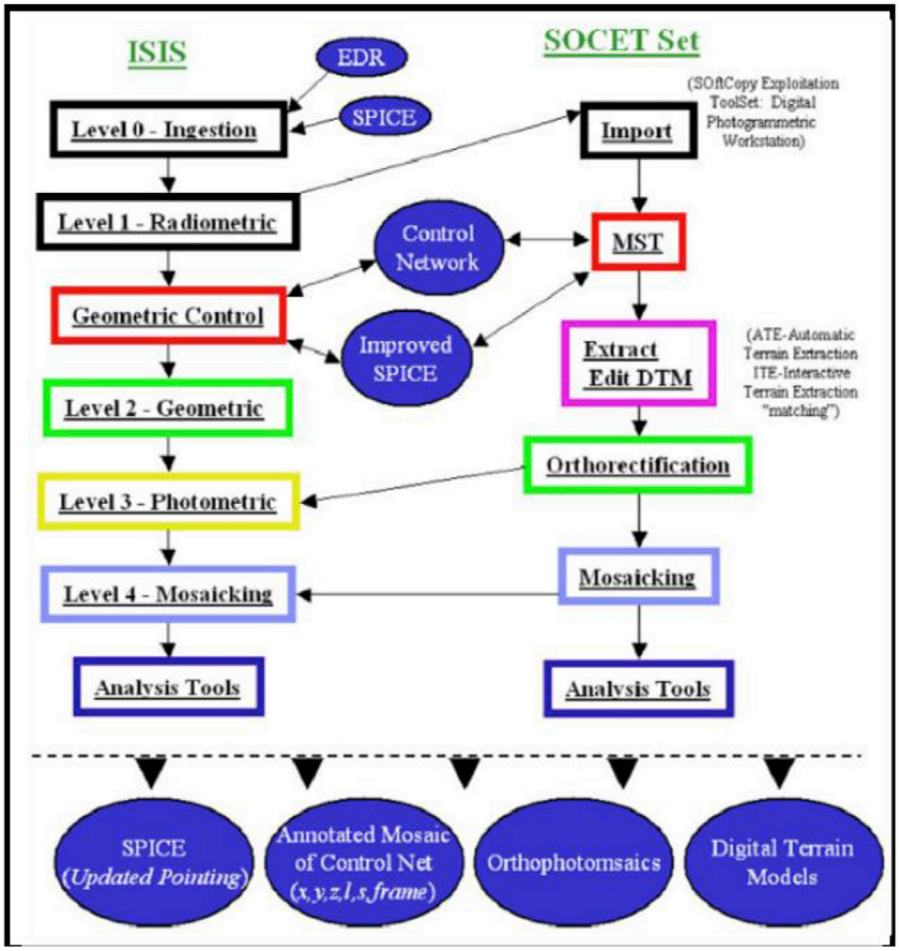

Fig. 2. Flowchart of ISIS and SS integration for topographic mapping (in general). Taken from the USGS Photogrammetry Primer document (page 12 at https://astrogeology.usgs.gov/search/map/Docs/Photogrammetry/Primer last accessed: 15.11.2017).

Table 1
Images used for the quality assessment.

	Instrument	IDs	ORI res.	DTM grid
MER-A	HiRISE	PSP_001513_1655 PSP_001777_1650	25cm	1m
	CTX	B18_016677_1653 G01_018523_1653	6m	18m
	HRSC	h4165_000_nd4.50 h4165_0000_dt4.50	12.5m	75m
MER-B	HiRISE	ESP_011765_1780 ESP_012820_1780	25cm	1m
	CTX	B22_018134_1779 G01_018490_1779	6m	18m
	HRSC	h1183_0000_nd4.53 h1183_0000_dt4.53	12.5m	100m
MSL	HiRISE	PSP_010639_1755 PSP_010573_1755	25cm	1m
	CTX	P21_009149_1752 P21_009294_1752	6m	18m
	HRSC	h1927_0000.nd4.52 h1927_0000.dt4.52	12.5m	50m

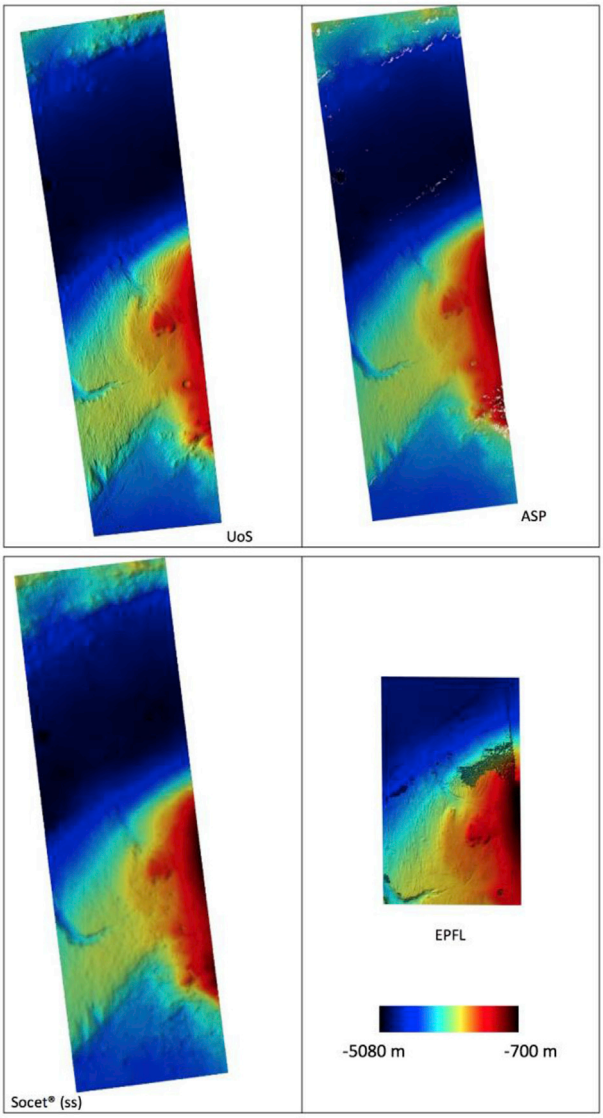

Fig. 3. Example of the 18m resolution DTM products for the MSL landing site used for comparing different DTM-algorithms: UoS, ASP, SS, EPFL. The same colour key (shown on the lower right panel) was used for the visualisation of these four DTMs. (For interpretation of the references to colour in this figure legend, the reader is referred to the Web version of this article.)

aka DTM generation), interactive terrain extraction (ITE; aka manual DTM editing) algorithms for stereo matching, multi-sensor triangulation (MST; aka BA) for geo-referencing, ORI generation, and mosaicking.

2.4. Quality assessment

Although on Mars, there is no "truth" (reference) DTM when comparing different automatically produced algorithms, but the inter-comparison of at least three different algorithms can indicate those DTMs which are consistent with each other and those which are not. In addition, we can compare multiple resolution DTMs from HRSC (50-150m), CTX (18m) and HiRISE (1m) over the same area with each other. In the early stages of the iMars project, pairwise comparisons of the DTM algorithms from ASP, SS, and two in-house pipelines developed by UoS and EPFL were performed by applying them to CTX stereo imagery for the rover landing sites on Mars (MER-A: 14.5718°S 175.4785°E; MER-B: 1.9462°S 354.4734°E; MSL: 4.5895°S 137.4417°E). The supporting DTMs and images were taken from the HRSC products overlapping with the CTX images. Additionally, some HiRISE stereo-pairs overlapping with the selected CTX images were also processed using the SS and the ASP system for comparison purposes.

The CTX DTM assessment was carried out first by checking how well each DTM set were co-registered with HRSC and how well each CTX DTM was co-registered with each other. The next step was generating pair-wise height differences and analysing the difference maps, histograms, and averages. The image IDs, scales of the images and DTMs from each pipeline for each site can be found in (Table 1). Examples of the colour hillshaded MSL DTMs from UoS, ASP, SS and EPFL pipelines are shown in (Fig. 3) and the difference maps of EPFL and UoS CTX product (P21_009149_1752_XI_04S222W and P21_009294_1752_XI_04S222W) with respect to the HRSC, ASP and SS products are shown in (Fig. 4 and Fig. 5). The reader should note the apparently lower resolution of the SS products in this and subsequent figures due to smoothing within SS. The mean differences (in metres) between the three data sets and the corresponding standard deviations are presented in (Table 2).

The comparison of multiple DTMs allows the establishment of the origin of the systematic differences between them. For example, for pairs with greater than 10 m differences in Table 2 correspond to the EPFL MSL DTM indicating that this product has a systematic offset with respect to the other data sets. Indeed, by analysing the difference maps for this

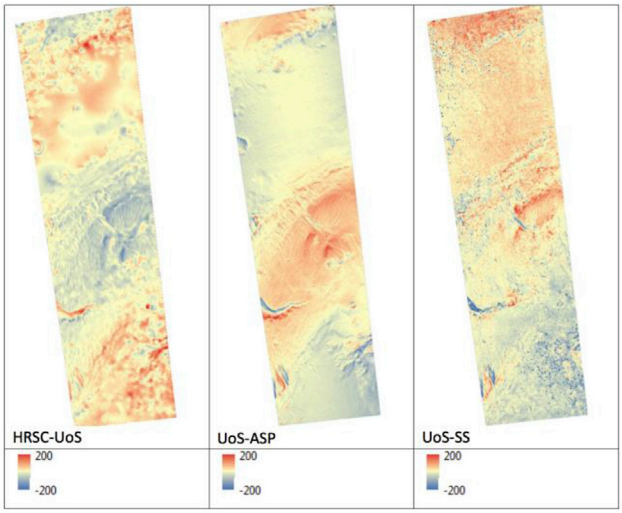

Fig. 4. Difference maps for the UoS MSL CTX DTM product obtained for the reference DTM products for the HRSC, ASP, and SS algorithms. The colour scale bar is given in metres. (For interpretation of the references to colour in this figure legend, the reader is referred to the Web version of this article.)

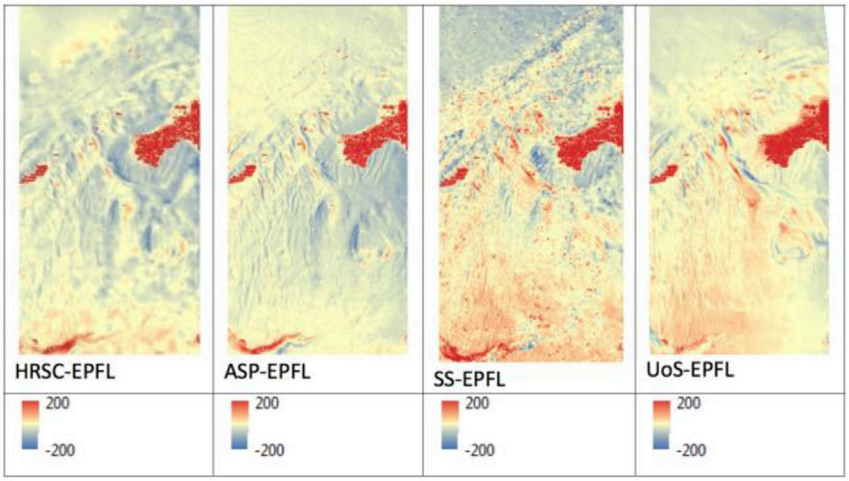

Fig. 5. Difference maps for the EPFL MSL CTX DTM product obtained for the reference DTM products for the HRSC, ASP, SS and UoS algorithms. The colour scale bar is given in metres. (For interpretation of the references to colour in this figure legend, the reader is referred to the Web version of this article.)

Table 2
Statistics of the height differences between the five MSL CTX DTMs compared with each other and their corresponding standard deviations.

DTM difference pairs	Mean difference (m)	St. Dev. (m)
HRSC-UoS	+1.4	84.2
HRSC-ASP	0.9	32.3
HRSC-SS	−1.3	56.5
HRSC-EPFL	−17.5	75.7
UoS-ASP	−2.1	84.4
UoS-SS	−2.7	84.9
UoS-EPFL	10.4	81.3
ASP-SS	−0.9	55.9
ASP-EPFL	−15.6	74.2
SS-EPFL	3.3	85.9

product (Fig. 5) one can find that the easternmost part of the MSL site valley in the EPFL DTM is systematically shifted up by about 200 m. The scatter plots for different difference combinations between the HRSC, ASP, SS, UoS, and EPFL DTMs together with the corresponding histograms for the DTM differences are shown in (Fig. 6 and Fig. 7).

Following this analysis, it was concluded that the ASP pipeline appears to perform better for the tasks of the iMars project than either SS, UoS or the EPFL pipelines, in terms of DTM quality and accuracy, when compared to the HRSC DTM products. In order to further examine the performance of the ASP pipeline, HiRISE DTMs were generated for the rover sites to compare against the CTX and HRSC DTMs. The mean differences between the HiRISE MSL DTM, three lower resolution DTMs (HRSC, CTX UoS, CTX ASP) and a HiRISE DTM produced by SS are presented in (Table 3).

All DTMs were produced relative to the MOLA sphere (3396.0m). The dispersion of the differences is small (12m) except for SS, which indicates the consistency of heights produced by the ASP for HiRISE. The differences with the three lower resolution datasets are all about 20 m (negative). The large dispersion of the differences is due to a larger number of surface features over a larger area for CTX and a smaller number of features for a smaller area covered by the HiRISE instrument. The standard deviations of the four comparison datasets are small, which shows that the preliminary pipeline for DTM production is working satisfactorily. However, the ASP results were considered to require improvement in global consistency, completeness and robustness in the working version of the DTM-generating software pipeline for iMars; therefore, an ASP variation was developed and used for the mass production of Mars DTMs. This variation, named CASP-GO, is described in the next section.

3. CASP-GO method

3.1. Defining non-repeat stereo pairs

Unlike HRSC and CaSSIS (Thomas et al., 2017), all other instruments acquiring high-resolution orbital imagery on Mars (including HiRISE and CTX) do not have a capability to capture single-pass stereo. Hence, HiRISE and CTX stereo pairs are composed of images acquired at different times and slew angle. Moreover, released lists for either HiRISE or CTX stereo pairs are incomplete. For example, the list of CTX stereo pairs only include images acquired rather early in the mission (https://raw.githubusercontent.com/zmoratto/Mars3DGearman/master/CTX_stereo_pair.txt last accessed 18.11.2017).

In order to extract full lists of stereo pairs, SPICE kernels and image metadata of the complete set of images acquired up to 29 February 2016 were employed. Due to limitations on the available computer resources, the goal was to estimate the most straightforward to process stereo pairs, i.e. those that map approximately the same region. Therefore, initially the image overlap ratio, defined as the rate of the common image area versus the area of the largest image, was used to estimate a preliminary set of overlapping image pairs. The overlap threshold was set to 90%. This would then only identify around one third of all possible stereo-pairs but ensure that stereo-pairs which might contain small pieces of images (i.e. slivers) which might overlap were eliminated (Cook et al., 1996).

Subsequently, overlapping pairs were examined according to their acquisition setup, following previously reported criteria used to declare a stereo pair (Cook et al., 1996). In particular, the imposed criteria use the following: (a) the 3-dimensional stereo angle between the two images must be larger than 8°; (b) the incidence angle in both images must be less than 89°; (c) the incidence angle difference must be less than 10° and (d) the solar longitude (i.e. the Ls) difference must be less than 45°. The first constraint clusters image pairs with the best detectable disparity, whilst the second discards images acquired near the terminator. The third constraint is used to avoid shadow effects while the final one is employed to ensure that seasonal changes do not affect the mapped scene. In a post-processing step, repeat CTX stereo pairs covering the same area are discarded, thus generating a list of unique CTX stereo pairs.

This approach generated a list of 3963 CTX stereo pairs all over Mars, which can be downloaded from the iMars website (http://www.i-mars.eu/publications/products/ctx last accessed: 15.11.2017). Subsequently, this process was repeated for HiRISE imagery, before imposing two additional constraints: (a) the HiRISE stereo pair must lie within a CTX stereo pair identified previously and (b) it must include an area that has been imaged at least 5 times by HiRISE imagery. The first additional criterion is essential for the stereo processing pipeline so that all geospatial co-ordinates are co-registered whilst the second is imposed due to

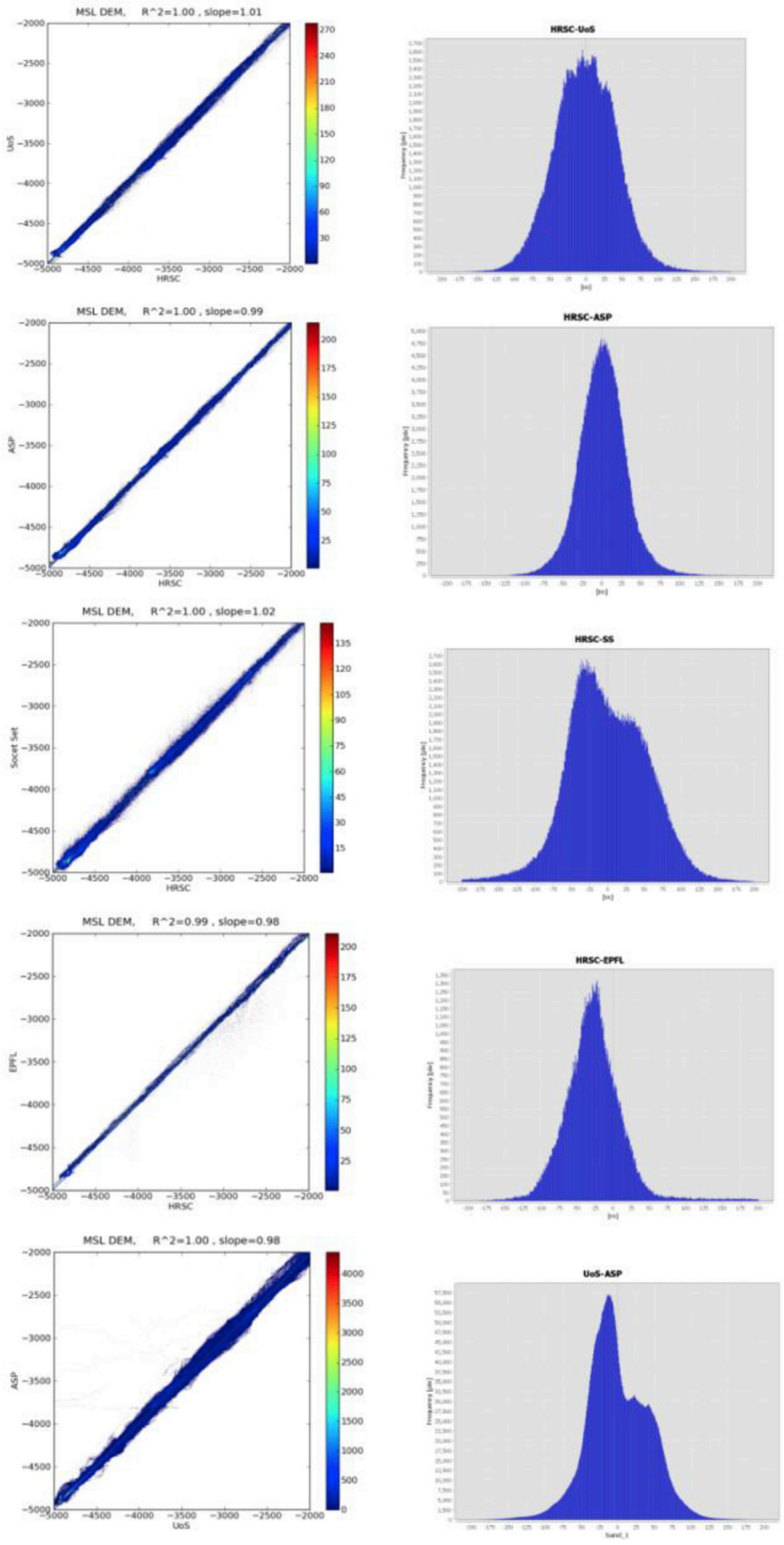

Fig. 6. Scatter plot indicating the correspondence between the MSL CTX DTMs generated by different pipelines together with the histogram for the difference map (part 1: HRSC-UoS, HRSC-ASP, HRSC-SS, HRSC-EPFL, UoS-ASP from up to down).

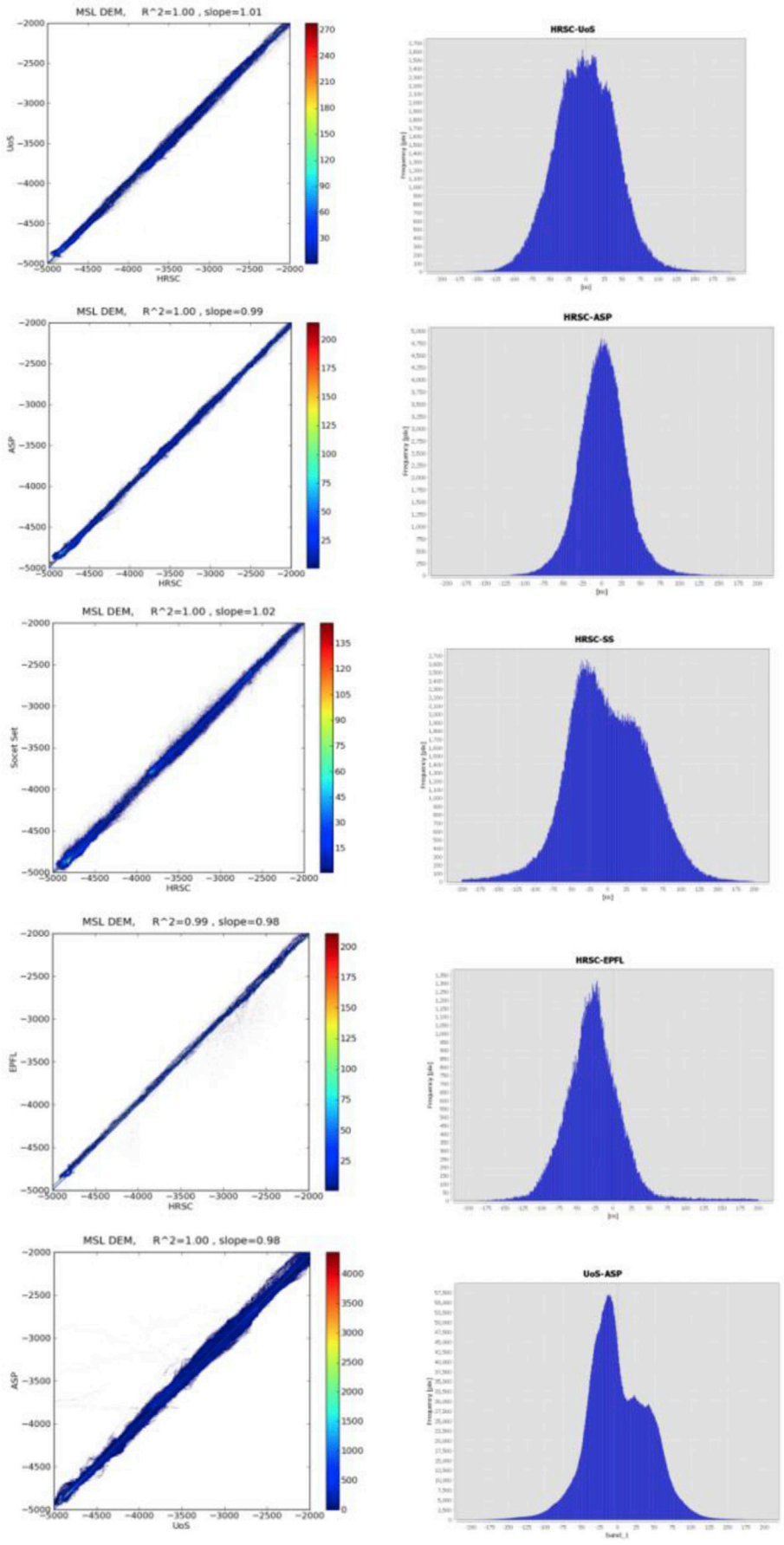

Fig. 7. Scatter plot indicating the correspondence between the MSL DTMs generated by different pipelines together with the histogram for the difference map (part 2: UoS-SS, UoS-EPFL, ASP-SS, ASP-EPFL, SS-EPFL from up to down).

Table 3
Statistics of elevation differences between the HiRISE DTM, HRSC DTM, UoS CTX DTM, ASP CTX DTM and SS HiRISE DTM corresponding to the same MSL test site area.

DTMs compared	Mean difference (m)	St. Dev. (m)
HRSC-ASP	−27.3	8.4
SS-ASP	65.3	12.7
ASP (CTX) – ASP (HiRISE)	−17.8	6.2
UoS (CTX) – ASP (HiRISE)	−21.2	10.4

computer resource limitations, so as to focus on regions where super-resolution restoration (Tao et al., 2016a) can be applied to HiRISE images. Discarding repeated stereo pairs generated a list of 441 HiRISE stereo pairs all over Mars, this can also be downloaded from the iMars website (http://www.i-mars.eu/publications/products last accessed: 15.11.2017).

3.2. CASP-GO pipeline overview

The CASP-GO pipeline is based on the ASP pipeline with enhancements from in house software previously developed. CASP-GO takes ISIS formatted "left" and "right" MRO images (HiRISE or CTX) and a reference HRSC ORI as inputs (CTX in the case of HiRISE DTM). It uses a combination of the ASP functions and the 5th generation of an adaptive least squares correlation and region growing matcher called Gotcha (Gruen-Otto-Chau) (Shin and Muller, 2012), which provides accurate and robust sub-pixel conjugate points. CASP-GO generates raster products such as ORIs and DTMs that are co-registered to either a previously processed CTX ORI and DTM or one generated from HRSC.

The complete CASP-GO workflow for CTX DTM production (Fig. 8) has the following 10 steps: (a) ASP "left" and "right" image pre-processing (image normalisation, Laplacian of Gaussian filtering, pre-alignment); (b) ASP disparity map initialisation (pyramid cross-correlation to build a rough disparity map); (c) UCL fast Maximum Likelihood (f-ML) matching and building of a "float" initial disparity map; (d) ASP Bayes Expectation Maximisation (BEM) weighted affine adaptive sub-pixel cross-correlation; (e) UCL refined outlier rejection gap erosion scheme to remove and eliminate mis-matched and unreliable disparity values; (f) UCL Adaptive Least Square Correlation (ALSC) based sub-pixel refinement; (g) UCL Gotcha (ALSC with region growing) based refinement and densification method to refine the disparity value and match un-matched or mis-matched area; (h) UCL co-kriging grid-point interpolation to generate ORI and DTM as well as height uncertainties for each DTM point; (i) UCL ORI co-registration/geocoding with reference to HRSC orthoimage and DTM adjustment. Optionally, (j) Generation of Object Point Cloud (OPC) using a remote server from our collaborator at Joanneum Research Institute for 3D real-time visualisation on a GPU using Pro3D®, primarily for HiRISE products (Traxler et al., 2017). Each of these function extensions/modifications (labelled as the UCL pipeline) will be discussed in more detail in the next section.

HiRISE images are 10–15 times larger than the corresponding CTX images and contain much richer fine scale features (at 25cm) that may vary in appearance from one stereo image to another. The HiRISE EDR products also contain systematic noise such as strip noise and gain variations. Based on the results from the experimental sites of MER-A, MER-B and MSL, several modifications (Fig. 9) were made to the original CTX CASP-GO DTM processing chain in order to produce the best possible results for HiRISE images.

Firstly, pre-processing is required for HiRISE images using routines from the USGS-ISIS processing suite. One important difference between HiRISE and CTX is that HiRISE is composed of multiple linear CCDs (Gupta and Hartley, 1997) that are arranged side by side with some vertical offsets (see (McEwen et al., 2007) for details). These offsets mean that the CCDs view the same terrain at a slightly different time and angle.

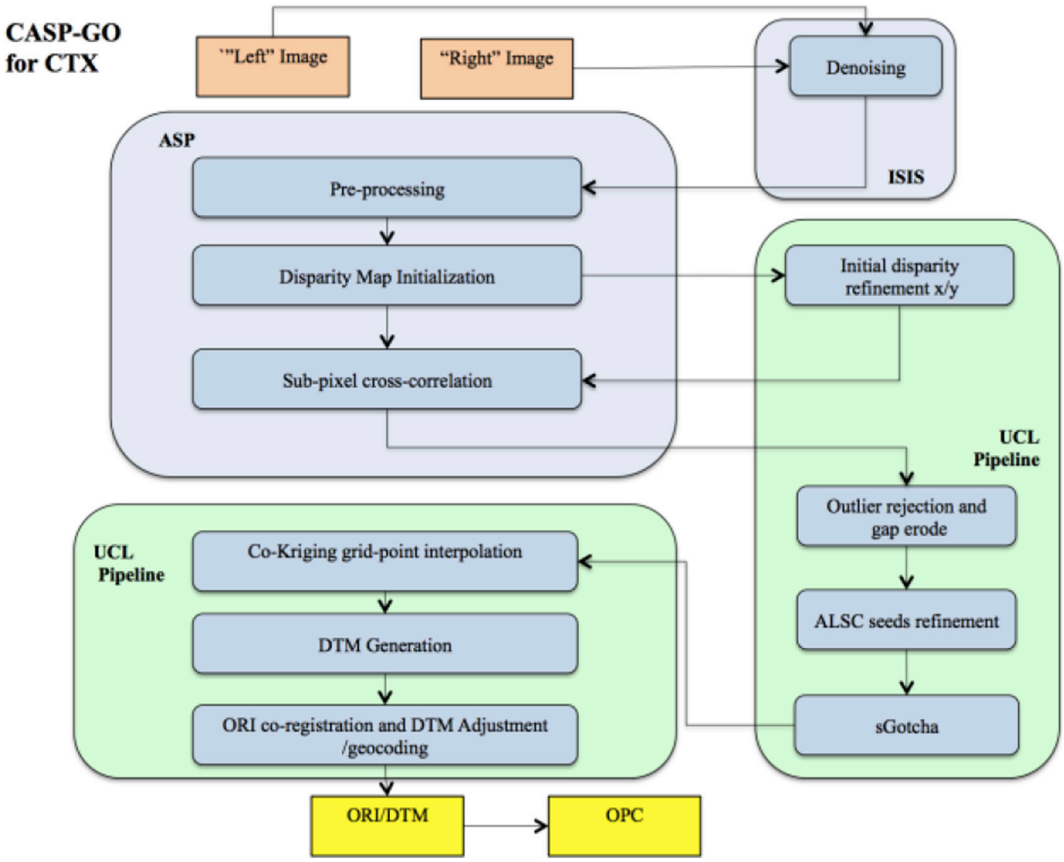

Fig. 8. Flow diagram of the UCL-ASP "CASP-GO" processing chain for CTX DTM processing.

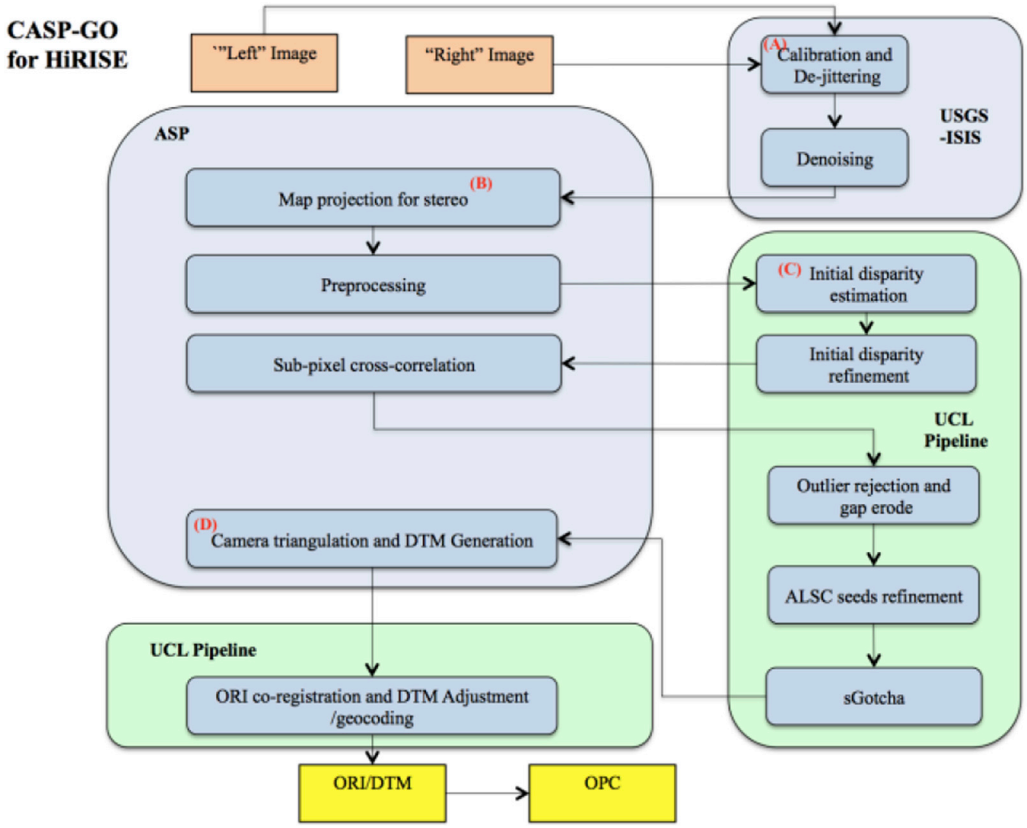

Fig. 9. Flow diagram of the UCL-ASP CASP-GO processing chain for HiRISE DTM processing.

The USGS-ISIS pre-processing steps in (Fig. 9) include the standard USGS-ISIS functions for HiRISE CCD radiometric de-calibration, stitching, SPICE kernel initialisation, and a de-jittering process. This is followed by a sequence of USGS-ISIS de-stripping and Kuwahara denoise filters (https://isis.astrogeology.usgs.gov/Application/presentation/Tabbed/kuwahara/kuwahara.html last accessed: 10.01.2018). This modification is labelled as (A) in (Fig. 9]. With respect to the jittering issue, we also worked with the University of Arizona HiRISE team to de-jitter specific HiRISE scenes.

Secondly, we found that the raw feature extraction algorithms from ASP are not accurate enough without further refinement, especially for image pairs that contain large topographic variations. This always leads to abnormal epipolar-rectification transformations. In this case, building upon the approach originally proposed by Kim and Muller (2009), we used the ASP's map projection to stereo function, which is an ASP wrapper based on USGS-ISIS functions, to remove the large disparity differences between HiRISE images and leave only a small disparity for estimation of initial disparity maps. This modification is labelled as (B) in (Fig. 9). This is similar to the approach previously proposed by (Kim and Muller, 2009). With USGS-ISIS formatted inputs, one can always work backwards through a map-projection when applying a camera model, so the geometric integrity of the input images should not be sacrificed if map-projection is applied first.

Thirdly, we use a block matcher based on the ASP's absolute difference initial disparity estimation method to calculate integer based disparities on a coarser scale. This directly compares the map-projected and x/y disparity minimised stereo images to generate a smoother initial disparity map with lower mismatches than cross-correlation. This modification is labelled as (C) in (Fig. 9). This step is still followed by the fast Maximum Likelihood refinement approach to generate sub-pixel level initial disparity map.

Finally, a less restrictive outlier rejection and erosion scheme is used. Note that the co-kriging steps are optional for HiRISE images due to their large image size and consequent very lengthy processing time. This modification is labelled as (D) in (Fig. 9).

In CASP-GO, we have developed a fully automated processing system with improved performance compared to the original ASP system. In particular, CASP-GO includes (a) co-registered geo-spatial coordinates with respect to HRSC (and MOLA) data; (b) improved DTM completeness for unmatched areas; (c) reduced DTM artefacts; (d) improved DTM accuracy; (e) fully documented uncertainties for every single interpolated height point. We now discuss these features in more detail.

The CASP-GO processing system was initially tested using CTX stereo images over both MER and MSL landing site, and subsequently over the MC11-E mosaic. Subsequently, it was streamlined to operate on cloud computing resources and has since been be applied to a large fraction of the global CTX stereo pairs (≈5500 pairs each) and some of the 441 stereo pairs of HiRISE. These products are available to the planetary science community as they are processed and quality controlled through the iMars webGIS and in the future through the NASA PDS system.

3.3. *Initial disparity refinement*

During our initial experiments, one of the major artefacts we found with the ASP results are a "staircase" effect in the overall DTM. This artefact can be observed clearly after performing a hill-shading process (illumination elevation 30° and azimuth 330°). The subsequent so-called "quilting" repeat pattern can be observed in (Fig. 10 and Fig. 11). The quilting pattern repeats are obvious using two different routines for their display at the same resolution of the first level of the pyramid, which is equal to the resolution of the initial disparity map. We found that even though the ASP BEM weighted affine adaptive correlation exhibits a high degree of robustness to image noise, refining the lower resolution integer disparity map still generates severe quilting patterns. This is referred to in the ASP documentation as the "pixel locking effect" and appears on both the faster ASP sub-pixel correlation solution, i.e. parabola fitting, and the slower sub-pixel solution, i.e. BEM weighted affine correlation. This is because the sub-pixel disparities tend towards their integer estimates.

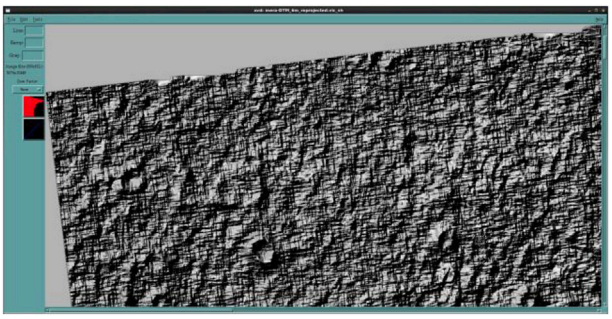

Fig. 10. MER-A 6m hill-shaded CTX DTM using the hwshade VICAR routine showing the staircase artefact.

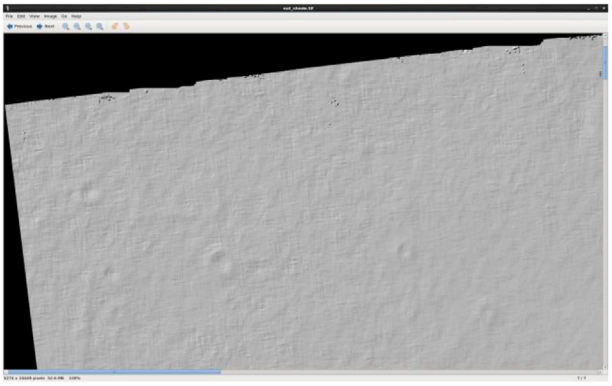

Fig. 11. MER-A 6m hill-shaded CTX DTM using the gdaldem GDAL routine showing the staircase artefact with less contrast.

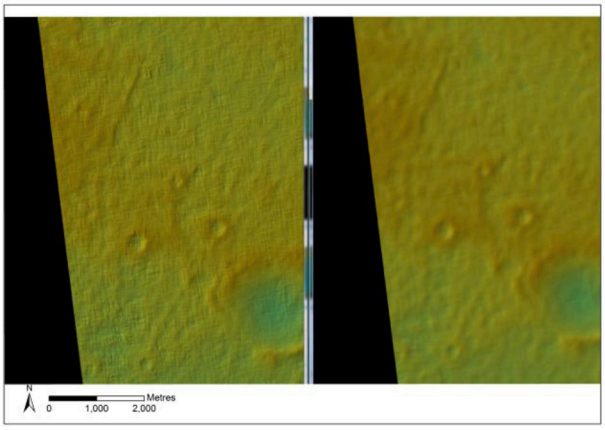

Fig. 12. An example of a colourised by height and hillshaded MER-A 18m CTX DTM, showing quilting artefacts from ASP processing (left) and the DTM after initial disparity refinement in CASP-GO (right).

Moreover, when using a lower resolution integer estimate, the ASP workflow doesn't guarantee continuity between sub-pixel disparities from different adjacent integer estimates. The "staircase" becomes more obvious in feature rich areas, e.g. at a crater edge, because the difference between two adjacent integer estimates is higher in these areas.

In order to reduce the "staircase" artefact, we can either generate integer disparity estimates at the same resolution as the final sub-disparities, or generate float disparity estimates at lower resolution. After experimentation, we applied a f-ML image matcher (Olson, 2002) to generate float disparity estimates at the same resolution as the ASP integer based correlation. The probabilistic formulation for lower resolution matching uses an arbitrary likelihood function for the matching error between edge or image features that eliminates the sharp distinction between matched and unmatched templates. In this approach, we search for maximum likelihood estimation of template positions, i.e. the joint probability density function (PDF) for the distances. The joint PDF is modelled as the sum of the error density when an edge pixel is an inlier and probability density of the distances when the edge is an outlier. Olson (2002) described a multi-resolution search strategy that examines a hierarchical cell decomposition of the space of possible template positions, which divides the space of template positions into rectilinear cells and determines recursively which cells could contain a position satisfying the acceptance criterion. In our case, given that we have already obtained integer distance estimates and in order to compute the PDF, only the magnitude of distances is required. The search strategy can therefore be simplified to find template positions in the 8 cardinal directions with a threshold equal to half of the difference of integer disparity value in each direction.

The maximum-likelihood measure gains robustness by explicitly modeling the possibility of outliers and allowing matches against pixels that do not precisely overlap the template pixel from cross-correlation. It is a fast and robust approach to turn ASP integer disparity to float initial disparity maps at a lower resolution, which are then used as seed disparities in ASP sub-pixel cross-correlation, i.e. the 4th step in the CASP-GO system. The results are displayed in the right-hand image of (Fig. 12). Most of the quilting artefacts have gone although there is still a slight residual displayed.

3.4. Outlier rejection and erosion scheme

Final sub-pixel disparity maps obtained from the refined initial disparity map still have various challenges for different input data. For example, from our experiments on the CTX DTMs for MER-B and MSL, two obvious problems are unmatched areas (no disparities available, i.e. errors of omission) and mismatched areas (wrong disparities, i.e. errors of commission). The first issue can be triggered in various situations: (a) input images have been acquired at very different Martian Solar Longitude (Ls) that has different lighting conditions; have different contrast or appear differently from different angles due to anisotropic scattering properties of the surface; (b) matching regions have very little texture or extremely low contrast such that there is insufficient signal to noise ratio and may be rejected during the correlation stage; (c) the regions of matching are highly distorted due to different image perspectives, such as crater and canyon walls. In addition, one or both of the input stereo-pairs might be affected by obscuration, such as dust clouds or the Ls is sufficiently different that features may be missing (e.g. polar regions).

The ASP correlation process attempts to find a match for every single pixel using a window that evaluates the lowest cost compared to all the other search locations. Generally, if we use a smaller search kernel and smaller search range, there will be more unmatched areas, giving more chances that the template in the left image cannot find any matched template in the limited search area in the right image. On the other hand, if the kernel is larger, then more areas can be matched but at the expense of losing fine-scale detail, because the disparity field tends to be too smooth. Moreover, selecting too large a search range increases the probability of false matches, i.e. cases when the template in the left image finds an erroneous "matched" template far beyond the true position with a lower correlation cost because the true position meets one of the situations listed above. The first issue thence becomes the second issue, i.e. mis-matches. Therefore, the kernel size and the search range needs to be selected as a compromise between the ratio of unmatched points to the ratio of the mismatched points, especially since both ratios impose significantly negative effects on the overall performance. More specifically, large unmatched areas can result in follow-on densification and co-kriging steps requiring extensively more computational time, while a lot of mis-matched points result in artefacts in the DTM. It is hard to eliminate all mis-matches even though we use a more accurate pre-allocated search range due to the innate weakness of cross-correlation and incorrectly matched seed points.

Consequently, in CASP-GO, a slightly larger correlation kernel is selected (75-125 pixels for CTX and 55-75 pixels for HiRISE), so as to minimise the extent of un-matched areas, along with a smaller search range, which will in turn minimise mis-matches but leave some high disparity areas un-matched. Then, by rejecting mis-matched areas, and eroding the borders of mis-matched pixels and un-matched pixel, this will leave only un-matched areas, since generally the matching quality is much lower at the neighbours of "bad" disparities. These un-matched areas are addressed by the follow-on Gotcha densification and co-kriging interpolation based on the ASP sub-pixel disparity output discussed in the next subsection.

The outlier rejection schemes (ORS) consist of: (a) a disparity value differing more than a threshold of a percentage of pixels in a kernel; (b) a kernel with a standard deviation higher than a threshold; (c) the difference of the mean value of a kernel and neighbouring kernel is higher than a threshold; (d) a kernel with a neighbouring kernel is rejected by a threshold percentage; (e) adjacent disparity values from (a), (b) and (c). Note that the outlier rejection schemes may also remove some disparities that are actually correct. However, this is rectified with higher precision matching in the next step (Gotcha densification).

3.5. ALSC refinement and gotcha densification

Starting with the "cleaned" sub-pixel disparity map, an ALSC refinement is performed on all the remaining disparity values iteratively. These refined disparity values are used as seed points for Gotcha densification (Shin and Muller, 2012). The Gotcha matcher that is based on ALSC and region growing is a very powerful tool, both robust and accurate, which in the past was used for full-image matching. However, for large stereo-pair processing, in the context of iMars, it is too slow for large-scale image matching since it tries to match every point iteratively and re-sort all seed points when a new point is matched. Hence, in our pipeline Gotcha is used only as a supplementary tool, so as to match the (assumed sparse) remaining points from the previous step of unmatched areas. Given sufficient numbers of sub-pixel disparities that pass the outlier rejection scheme, small difficult regions can be matched accurately with Gotcha. For example, the geometrical distortion generated from different viewing angles can be addressed with Gotcha by iteratively modifying the shape of the ALSC window.

The Gotcha algorithm applied in this work can be summarised as follows: (a) with given sub-pixel disparity values, retrieve seed tie-points (point correspondences) on the border (within a 5 to 11 pixel width) according to the x and y translation (disparity); (b) run ALSC on the seed tie-points and store the similarity value; (c) sort seed tie-points by similarity value; (d) a new matching is derived from any adjacent neighbours of the initial tie-point with the highest similarity value; (e) if the new match is verified by ALSC then it is considered as a seed tie-point for the next region-growing iteration; (f) this region growing process repeats from (c) to (e) until there are no more acceptable matches; (g) retrieve the final disparity map after densification.

With Gotcha densification, improved completeness in the final DTM can be achieved without significantly smoothing out sharp features by applying a large matching kernel. Generally, a larger ALSC window and eigenvalue yields better completeness in disparity and hence DTM. See (Fig. 13) for an example of this. The similarity values from Gotcha matcher are then used together with co-kriging parameters to produce DTM uncertainty values (not shown here) (see Fig. 14).

3.6. Speeded up implementation of gotcha (sGotcha)

Due to the computational complexity of Gotcha densification software, further work is required to speed-up Gotcha. The starting point was a variation of the 4th generation of Gotcha implementation developed within the PRoVisG (Paar et al., 2012) and HiTES3D project (https://www.era-learn.eu/network-information/networks/eurostars/eighth-eurostars-cut-off-01-march-2012-20h00-c-e-t/high-temperature-environment-3d-stereo-measurement-for-corrosion-monitoring last accessed: 15.11.2017). Speeded up Gotcha (sGotcha) is an optimised (5th generation) version of Gotcha with improved single-threaded ALSC performance and more efficient handling of the tie-point queue. Region growing is performed by a number of worker threads which process the tie-point queue in parallel (Veitch-Michaelis, 2016).

Previously, a tiled approach was used for region growing. While this lends itself well to geometric parallelisation, as each tile can be processed independently, additional logic is required to avoid disparity discontinuities at tile boundaries. sGotcha does not use a tiled approach. All tiepoints are stored in a thread-safe, priority queue, ordered by match confidence. This removes the need to re-sort each time a new tie-point is added. Each worker thread de-queues the current best tie-point, performs ALSC refinement and, if it is a match, adds its neighbours to the queue. A thread-safe map of visited pixels is updated throughout the matching process to avoid repetition of the work. As with standard Gotcha, processing is finished when the tie-point queue is exhausted.

ALSC contains two particularly computationally expensive steps: the formation and inversion of the design matrix (Griin, 1985) and the interpolation of the right image during patch deformation. Cholesky decomposition (implemented using the Eigen library) is used to efficiently obtain a pseudo-inverse, and the bilinear interpolation code has been optimised. With these changes and numerous smaller optimisations throughout the codebase, the performance of each ALSC iteration was improved by almost an order of magnitude.

Overall this results in a near-linear speedup on multi-core CPUs and near-100% CPU utilisation during matching. On an Intel 6700K 4GHz processor with 8 logical cores, performance of around 1 min per Megapixel is achievable. Further single-thread improvement is possible by taking advantage of Single Instruction Multiple Data (SIMD) or vectorised instructions available on modern processors.

3.7. Co-kriging interpolation

After Gotcha densification, ideally, we should get disparities for most of the pixels. However, for some textureless or extremely low contrast

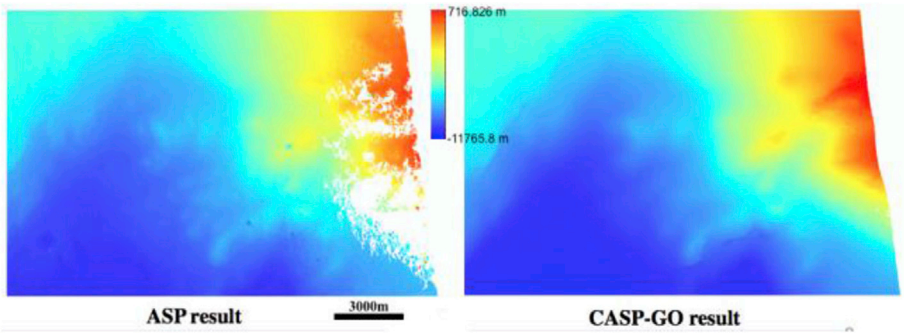

Fig. 13. An example of MSL DTMs derived from CTX stereo, showing un-matched areas from ASP processing (left) and improved completeness using Gotcha densification in CASP-GO (right).

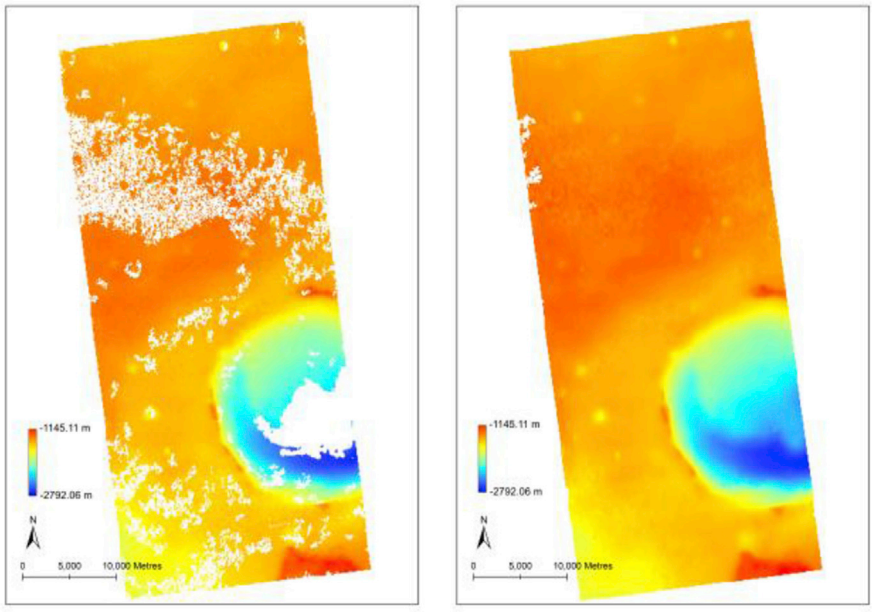

Fig. 14. An example of a MER-B DTM after bad matching rejection in CASP-GO (left) and the final DTM using Gotcha densification and co-kriging.

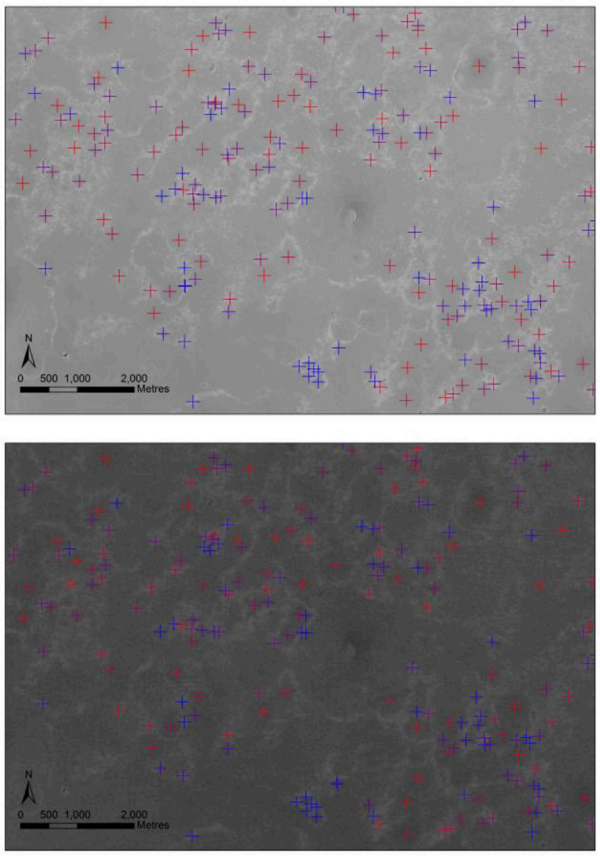

Fig. 15. An example of MSA-SIFT tie-points from MER-B CTX ORI (top) and HRSC ORI (bot), showing increasing uncertainty value from blue to red. (For interpretation of the references to colour in this figure legend, the reader is referred to the Web version of this article.)

areas, where the matching is rejected by both cross-correlation and Gotcha, the final DTM may still contain gaps. In this work, we use the co-kriging method to interpolate onto a gridded DTM. Kriging is a robust technique that uses a spatial model to bias the interpolation process.

Table 4
Image IDs employed for the experimental sites.

	"Left" Image ID	"Right" Image ID
MER-A CTX	B18_016677_1653 _XN_14S184W	G01_018523_1653 _XI_14S184W
MER-B CTX	B22_018134_1779 _XN_02S005W	G01_018490_1779 _XN_02S005W
MSL CTX	P21_009149_1752 _XI_04S222W	P21_009294_1752 _XI_04S222W
MER-A HiRISE	PSP_001513_1655	PSP_001777_1650
MER-B HiRISE	ESP_021747_1780	ESP_022380_1780
MSL HiRISE	ESP_018854_1755	ESP_018920_1755
Mars2020 HiRISE	ESP_047119_1560	ESP_047185_1560

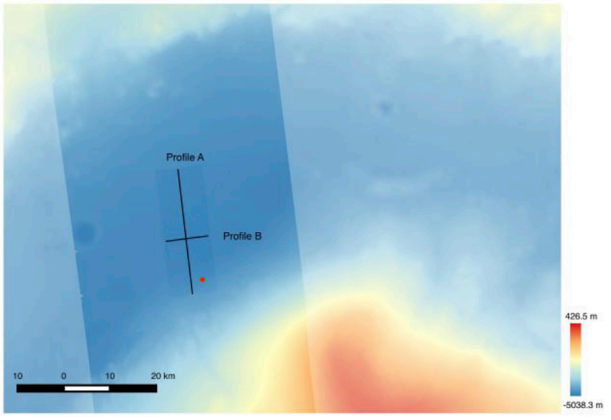

Fig. 16. An example of co-registered CASP-GO CTX (70% transparency) and HiRISE (100% transparency) DTMs displayed on top of the HRSC DTM H1927_0000_DT4 (50% transparency) for the MSL site at Gale Crater, showing good visual DTM completeness and co-registration accuracy spatially and vertically to HRSC v50 + product. Two profile lines (A & B) are labelled on the map. The red-dot is the location for the zoomed-up view of the HiRISE/CTX/HRSC ORIs is shown in (Fig. 17]. (For interpretation of the references to colour in this figure legend, the reader is referred to the Web version of this article.)

Kriging in DTM interpolation applications uses a weighted average, which depends on both the distance of point pairs and spatial variation, of neighbouring known elevation values to predict a missing elevation

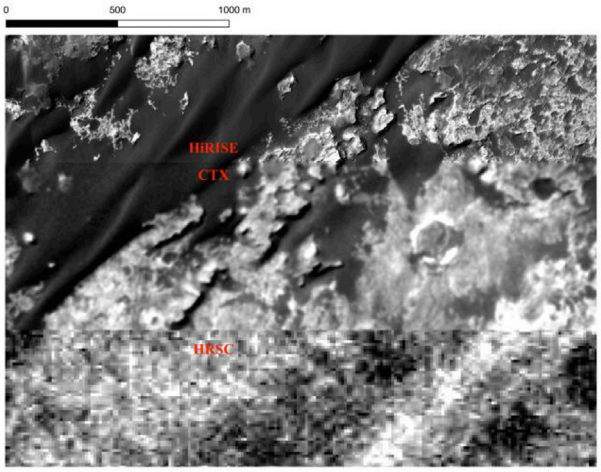

Fig. 17. A zoomed-up view of the corresponding 25cm HiRISE, 6m CTX, and 12.5m HRSC ORIs showing spatial co-registration quality for a random location indicated by the red dot in (Fig. 16). (For interpretation of the references to colour in this figure legend, the reader is referred to the Web version of this article.)

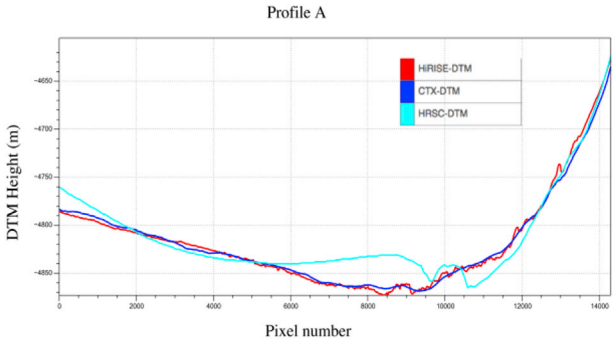

Fig. 18. Profile A for the multi-resolution MSL HiRISE-CTX-HRSC DTMs at Gale Crater.

value. A detailed description of the Kriging method can be found in (Stein, 1999).

In CASP-GO, a co-kriging method has been integrated using the open source Geostatistics Template Library (GsTL)'s C++ co-kriging implementation. Co-kriging is a computationally expensive algorithm. It is impractical to repeatedly solve the Kriging equations using all observations available. Therefore, a fixed search radius for determining neighbouring points has been used in CTX DTM interpolation. Also, the total size of interpolation needs to be minimised from the stereo matching and Gotcha densification steps. Nevertheless, co-kriging greatly improves the accuracy over linear facet interpolation of a Delaunay triangulation of the data and provides unique accuracy estimates for each and every point interpolated based on the estimated quality of the data. These are derived from the ALSC similarity measure, the camera model geometry and the spatial variation of the terrain (Day and Muller, 1989).

Each elevation pixel output from stereo matching is associated with various parameters, which may correlate with the elevation accuracy. These include the maximum eigenvalue of the covariance matrix that reflects uncertainty in the positioning of the matching window, a measure of the local consistency of line disparities, and optionally parameters of radiometric gain and shift, and skewness from the camera model.

On the other hand, the two rays from the camera perspective centre to an object point location never intersect perfectly at a 3D point in practice. This is because any slight error in camera position or orientation information will affect the camera ray positions. When taking the closest point of intersection of the two rays as the location of 3D from ASP disparity to point clouds triangulation, the actual distance between the camera rays at the point becomes an important elevation accuracy parameter. The distance between the two rays at their closet point of intersection is also a weighted term of the final uncertainty value. This is known as the skewness term.

3.8. ORI Co-registration and DTM adjustment

The refined stereo matching workflow has brought the CTX and HiRISE DTM production to an unprecedented level of accuracy and completeness. However, the HiRISE and CTX datasets are generally not co-registered with the HRSC ORI/DTM (DLR processed v50 products) and consequently through to the MOLA dataset. This was reported in a

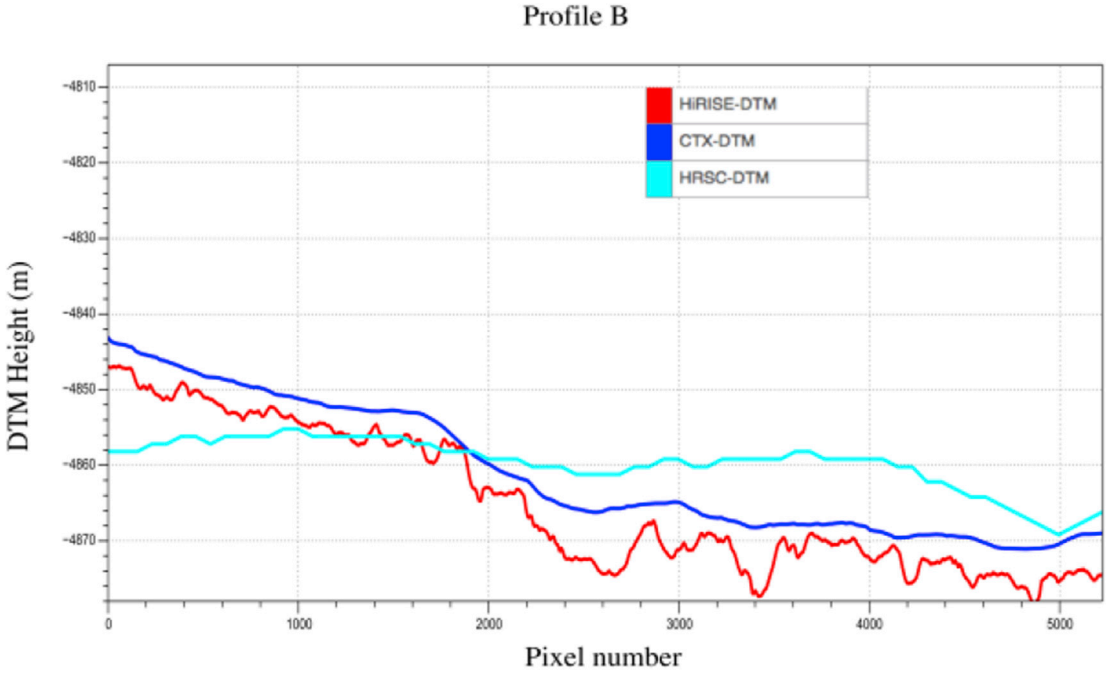

Fig. 19. Profile B for the multi-resolution MSL HiRISE-CTX-HRSC DTMs at Gale Crater.

previous EU project – PRoVisG and follow-on HiRISE-CTX-HRSC co-registration work in (Tao et al., 2016b). These mis-registrations can reach up to 100-200m between HiRISE/CTX and HRSC for the MER and MSL areas, according to the positions of manually selected control points on obvious landmark features, such as crater edges.

In this work, we have added the Mutual Shape Adapted Scale Invariant Feature Transform (MSA-SIFT) based co-registration workflow to the final ORI and DTM product. Technical details of MSA-SIFT and the evaluation on ORI/DTM co-registration results for MER and MSL are described in (Tao et al., 2016b). In this ORI co-registration and DTM adjustment work, we take the HRSC ORI as the reference image for CTX ORI co-registration (Fig. 15) and subsequent shift of the CTX DTM according to the CTX ORI to HRSC ORI transformation. For HiRISE co-registration, we take a co-registered CTX ORI as the reference image for HiRISE ORI co-registration and subsequent transformation of HiRISE DTM. It is also possible to use a CTX ORI as a base if it was previously processed and co-registered to HRSC.

Bringing all CASP-GO products into a unique geo-spatial context with respect to HRSC and MOLA data is important for subsequent data exploitation such as visualisation, GIS and change detection, which are the main goals in iMars.

3.9. UCL ACRO system

Apart from the cited co-registration software that has been mainly used in this work, an alternative is to replace it with another in-house automatic co-registration and orthorectification software (Sidiropoulos and Muller, 2017). The main novelty of this software is that it can automatically achieve sub-pixel co-registration of images that were acquired under significantly different imaging setups, including different slew angles and image quality. This co-registration software has been extensively tested on large volumes (~15,000) of high-resolution Mars orbital imagery and was used in a pre-processing step to achieve a first geometric alignment of the image pairs.

This automatic co-registration technique starts with point matching, in which SIFT features (Lowe, 2004) are matched to generate a set of tie-points. The main contribution of this algorithm lies in the fact that image matching is not conducted exclusively in the feature space, but it also includes geometrical constraints to reduce the required computational time by 2-3 orders of magnitude, while increasing the number of tie-points by 1-2 orders of magnitude. In the original automatic co-registration algorithm (Sidiropoulos and Muller, 2015) the tie-points determine a linear pushbroom camera model that finally produces the co-registered image. However, in the case of stereo processing, this resampling may have detrimental effects on the stereo quality. Hence, a less elaborate approach is followed, in which a global translation is estimated from a set of tie-points, and used to correct the image position without resampling it. It should be noted that in (Sidiropoulos and Muller, 2017) it was experimentally shown that a global translation is enough to reduce the mis-registration error from 40 to 5 pixels, for CTX images. More information about the automatic co-registration algorithm can be found in (Sidiropoulos and Muller, 2017).

4. Results

4.1. CASP-GO DTMs over MER, MSL, Mars2020 landing sites

The CASP-GO system was assessed independently by two sources: a data validation test performed by DLR and webGIS interface tests performed by FUB. Following these feedbacks, several key changes in the pipeline took place so the final output products would be in line with the required data quality, to reduce the processing time and to be compatible with the web-GIS interfacing requirements made by different partners within iMars. The CASP-GO outputs include a DTM, ORI, Gotcha "mask", co-kriging "mask", uncertainty map and hill-shaded colourised browser products, which can be directly ingested into the iMars web-GIS server.

In the development stage, the CASP-GO processing chain has been tested/applied to stereo CTX and HiRISE imagery over the MER-A, MER-B, MSL and one of the Mars2020 landing site candidates at Eberswalde. The images used in this experimental processing are summarised in (Table 4). The output product resolution is 18m for the CTX DTMs and 0.75m for HiRISE DTMs, while they were map-projected using the sinusoidal projection system with the same central meridian value as the corresponding HRSC v50 + single strip DTMs.

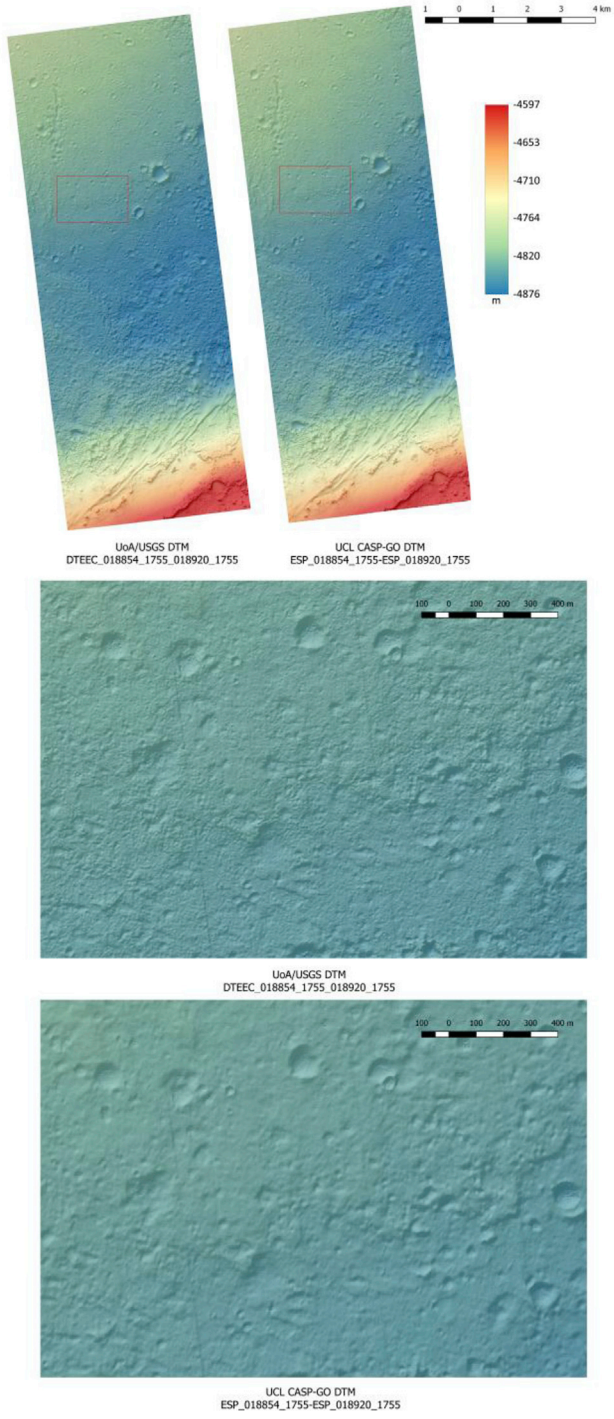

Fig. 20. Example of the MSL HiRISE DTM produced by CASP-GO compared to the UoA/USGS HiRISE DTM for the same area. The location of the zoomed-in views is shown in the red bounding box of the original DTMs. (For interpretation of the references to colour in this figure legend, the reader is referred to the Web version of this article.)

In (Fig. 16), an example of the 18m CASP-GO CTX DTM and 75cm CASP-GO HiRISE DTM superimposed on top of the 50m DLR HRSC DTM with different layer transparency is shown. A zoom-up view of the corresponding 25cm HiRISE, 6m CTX, and 12.5m HRSC ORIs showing spatial co-registration quality for the random location shown as the red dot in [Fig. 16] is given in (Fig. 17). Two profiles are shown in (Fig. 18 and Fig. 19). The maximum/average differences between CTX and HRSC for Profile A and B are 45m/10.5m and 17m/5m, respectively. The maximum/average differences between HiRISE and CTX for Profile A and B are 12.5m/3.5m and10m/2.5m, respectively. The maximum difference is partially subject to large spatial resolution differences between HiRISE, CTX and HRSC.

An example of the HiRISE DTM elevation profile in comparison with the UoA/USGS HiRISE DTM is also given in (Fig. 20). They are both of similar visual quality and completeness. Both of them have few thin strips coming from the original HiRISE image stitching. For a comparable flat area, the CASP-GO DTM is less noisy but the UoA/USGS DTM may contain more details.

At the experimental stage of HiRISE DTM production, two additional HiRISE DTMs at Eberswalde (Mars2020 candidate landing site) were processed using CASP-GO requested by collaborators at Imperial College (S. Gupta, private communication, 2017). The DTM and ORIs are shown in (Fig. 21 and Fig. 22).

As a result, all CTX and HiRISE datasets can be considered to be co-registered to the MOLA dataset as HRSC derived data are co-registered to MOLA (Gwinner et al., 2009; Gwinner et al., 2016). We have validated the DTM products of CASP-GO with respect to the quality of the resolved detail and quality of co-registration to HRSC. However, due to

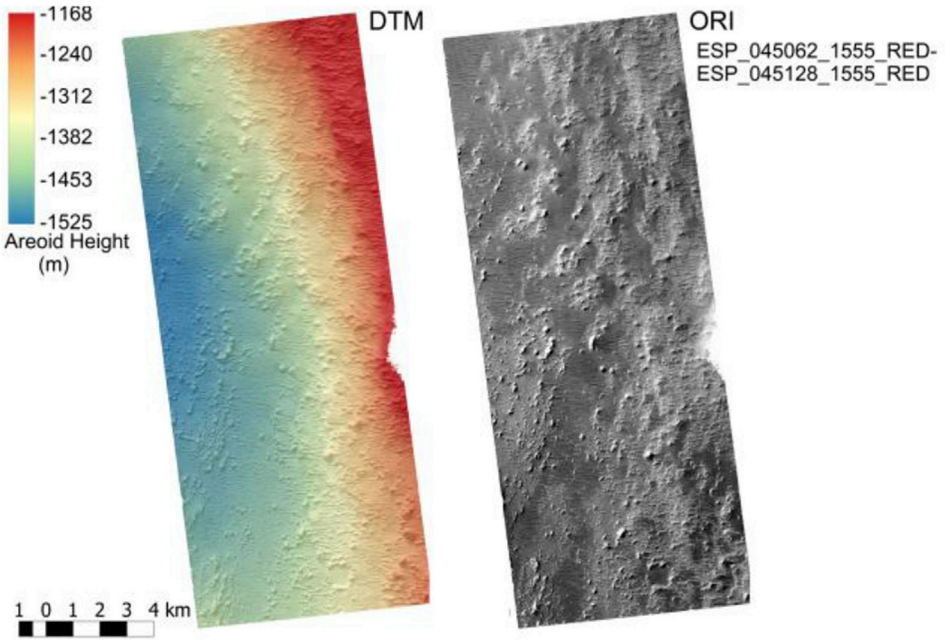

Fig. 21. Processed HiRISE DTM and ORI for one area within the proposed Mars2020 candidate landing site at Eberswalde.

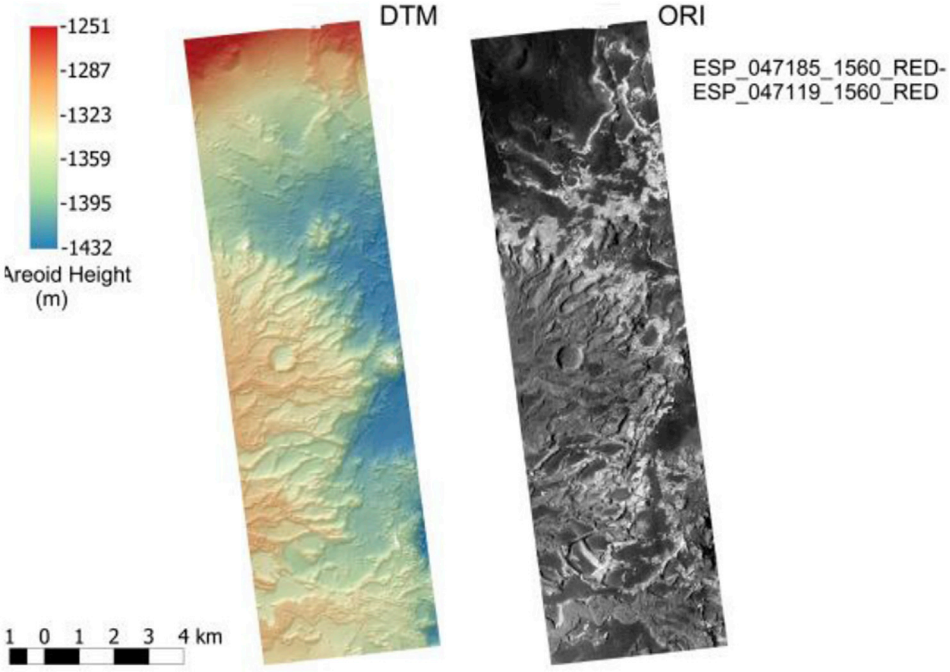

Fig. 22. Processed HiRISE DTM and ORI for one area within the proposed Mars2020 candidate landing site at Eberswalde.

Table 5
Statistics of CASP-GO CTX DTMs.

	Statistic Items	HRSC	CTX	HRSC-CTX
MER-A	No. of Elements	4,593,037		
	Minimum (m)	−3891.83	−3951.59	−121.331
	Maximum (m)	−3362.11	−3330.80	125.094
	Height range (m)	529.72	620.79	246.425
	Avg. DN value (m)	−3678.36	−3672.06	−6.29933
	Std Deviation (m)	46.6395	54.9509	17.7338
MER-B	No. of Elements	4,629,429		
	Minimum (m)	−2445.93	−2458.73	−540.707
	Maximum (m)	−1690.43	−1285.77	143.094
	Height range (m)	755.50	1172.96	683.801
	Avg. DN value (m)	−1946.81	−1972.58	25.7694
	Std Deviation (m)	129.835	122.475	22.8423
MSL	No. of Elements	7,072,512		
	Minimum (m)	−5339.23	−4983.46	−499.283
	Maximum (m)	−993.202	−1000.06	691.821
	Height range (m)	4346.028	3983.4	1191.104
	Avg. DN value (m)	−3623.88	−3625.72	1.838
	Std Deviation (m)	946.427	950.700	49.105

Table 6
Statistics of CASP-GO HiRISE DTMs.

	Statistic Items	CTX	HiRISE	CTX-HiRISE
MER-A	No. of Elements	88,182,234		
	Height range (m)	101.63	120.84	126.348
	Avg. Height (m)	−3688.85	−3669.31	−19.539
	Std Deviation (m)	14.078	14.056	5.851
MER-B	No. of Elements	53,853,617		
	Height range (m)	81.07	338.44	352.922
	Avg. Height (m)	−1883.53	−1883.57	0.0468
	Std Deviation (m)	10.317	11.401	7.745
MSL	No. of Elements	141,207,925		
	Height range (m)	379.01	404.49	128.277
	Avg. Height (m)	−4813.33	−4812.86	−0.464
	Std Deviation (m)	61.255	64.634	5.001

the wide range of resolutions from several hundred metres in the MOLA dataset to sub-metre resolution in HiRISE data, co-registration is always validated against the next lowest level of available resolution, e.g. HiRISE (25cm resolution in ORI) co-registration are tested against CTX (6m resolution in ORI). CTX ORI and derived data products are also compared against HRSC images and data products.

Several tests were made to validate the experimental DTM products. The tests are comparable to methods applied by (Heipke et al., 2007). Though the template data here are the HRSC and CTX derived products, these are compared and subsequently HiRISE is compared to CTX. Also, since the test areas are the rovers landing site areas only a few craters can be found in this data. Qualitative performance evaluation includes a) inspection of shaded relief for qualitative assessment of resolved detail, noise characteristics, and height artefacts and surface patterns; b) colour

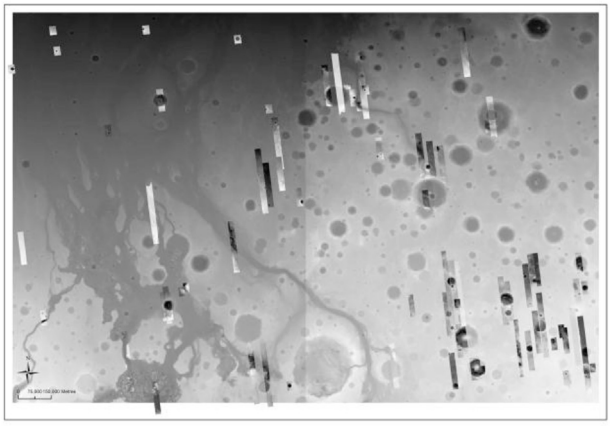

Fig. 24. Example of all unique CTX DTMs over MC11-E/-W area superimposed on the HRSC DTM mosaic basemap using QGIS.

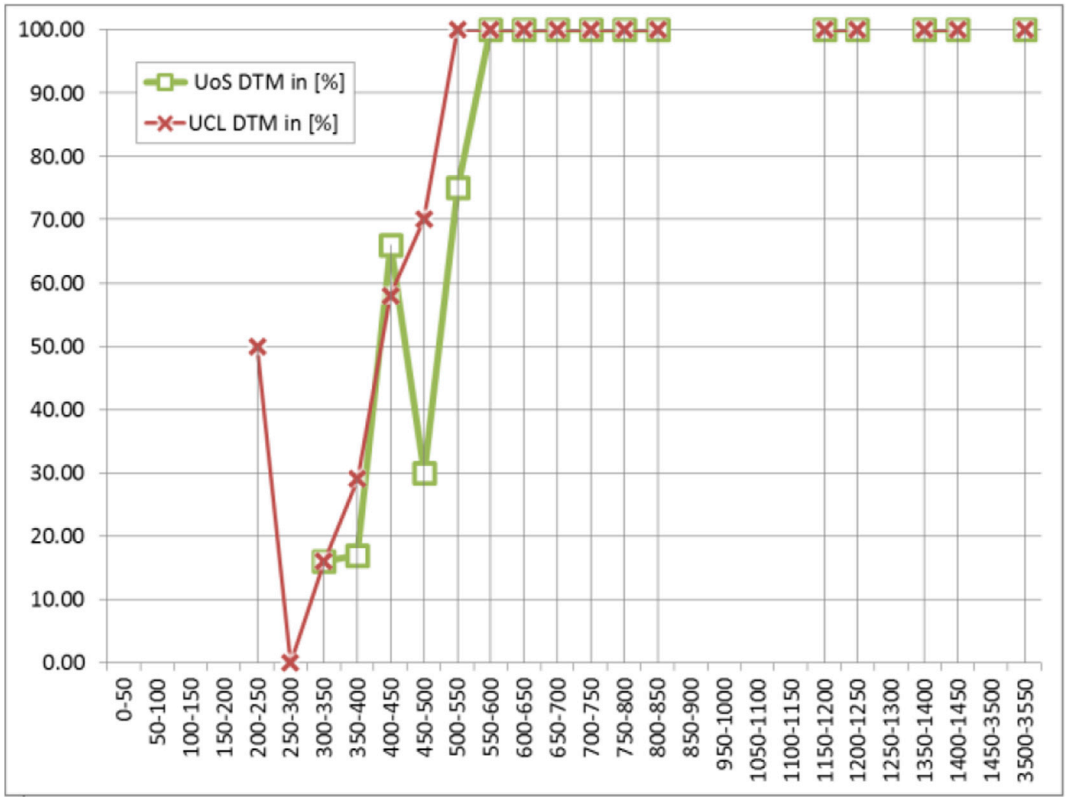

Fig. 23. Effective resolution estimation as observed in the CASP-GO CTX DTM and UoS DTM for MSL landing site area. Taken from iMars report D4.5 Validation of CTX and HiRISE DTMs (http://www.i-mars.eu/publications/imars-publications/d4-5 last accessed: 15.11.2017).

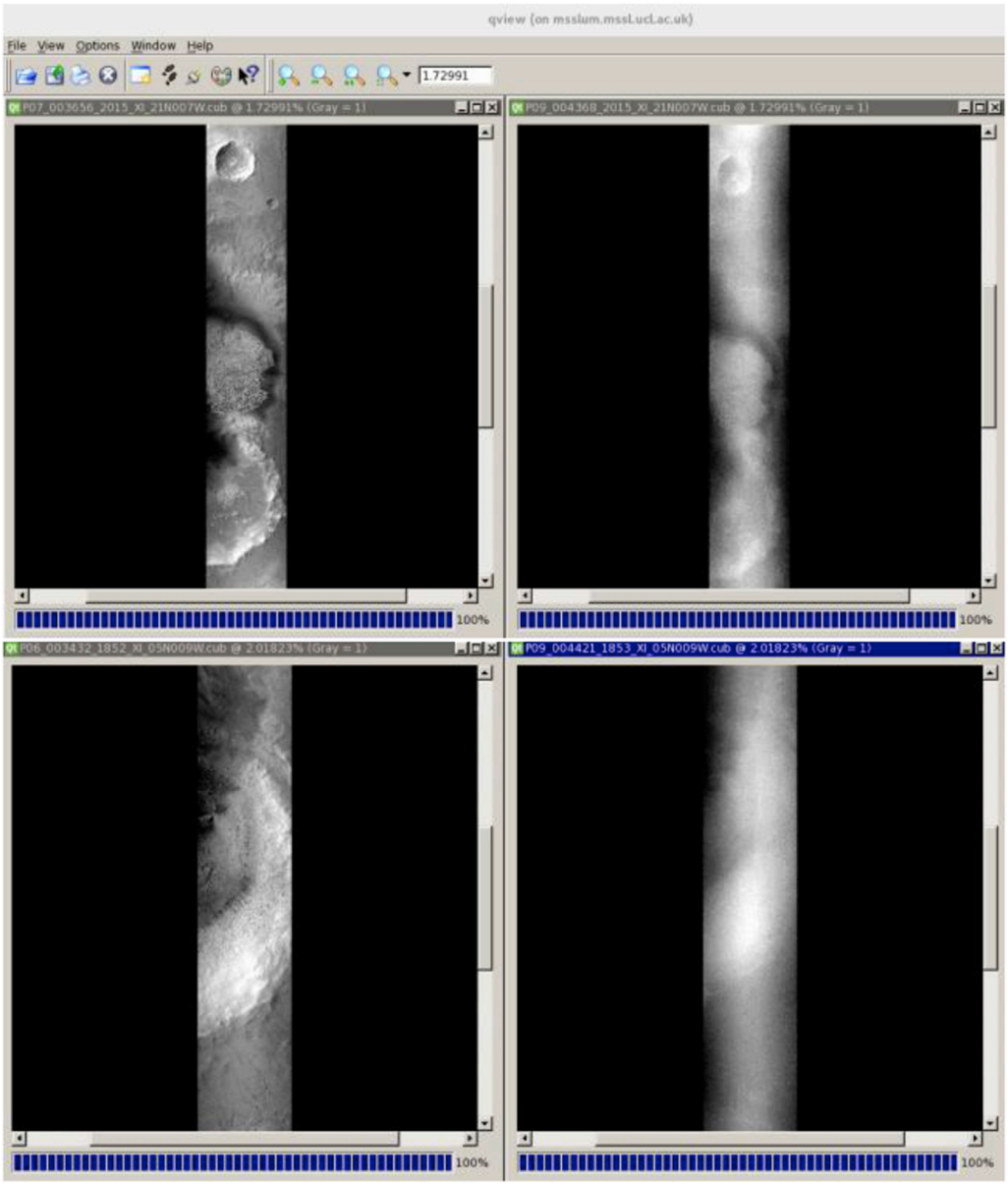

Fig. 25. Examples of failed CTX stereo pairs over MC11-E area showing poor input quality for the right part of the stereo-pairs.

Table 7
Image IDs of a subset of the co-registered HiRISE-CTX-HRSC DTMs at Ares-Vallis.

	Image ID
HiRISE	ESP_012939_1875
	ESP_012794_1875
CTX-1	D04_028921_1864_XI_06N018W
	D05_029066_1864_XI_06N018W
CTX-2	F16_042068_1881_XI_08N019W
	F16_042213_1880_XI_08N019W
HRSC	MC11E

coded overlay for visualisation of gross artefacts and internal model deformation and lateral shifts, but not suited for fine detail; c) evaluation of DTM height representation in comparison with visible surface features in the ORI. On the other hand, quantitative performance evaluation includes a) height difference statistics of the DTMs (minimum, maximum, and standard deviation values of height differences) in comparison to the reference HRSC DTM; b) crater statistics for selected data sets for effective resolution of the DTM – comparison of craters visible in the ORI and in the DTM.

The height statistics of CASP-GO CTX DTMs for MER-A, MER-B, and MSL are shown in (Table 5). The height statistics of CASP-GO HiRISE DTMs for MER-A, MER-B, and MSL are shown in (Table 6).

In order to derive a number for the effective resolution, craters in the CTX ORI were identified and measured and counted according to their crater size. Subsequently, the same craters were identified in the shaded DTM data and, if recognizable, counted into different classes of crater diameters. However, the derived statistics are just an indication of the effective resolution. This is due to the paucity of craters in the landing site areas, which is usually an engineering constraint for planetary mission due to safety concerns. The MSL landing site area was the only test site of the three considered sites, to provide a sufficient distribution in the crater diameter (http://www.i-mars.eu/publications/imars-publications/d4-5 last accessed: 15.11.2017).

In (Fig. 23), the graph shows the percentage of craters recognizable in the respective DTM with the reference of the crater counts in the ORI. It shows a comparison of the CASP-GO system and a competitive in-house DTM pipeline developed by the UoS (Kim and Muller, 2009) within the iMars project. It shows that craters in the diameter range between 400

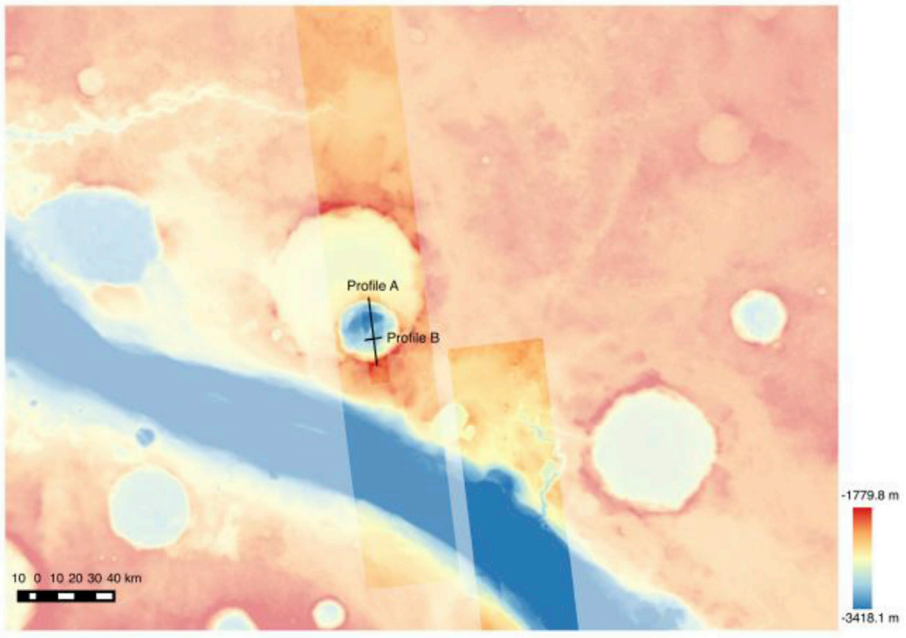

Fig. 26. Co-registered CASP-GO CTX (70% transparency) and HiRISE (100% transparency) DTMs showing on top of the HRSC MC11-E DTM (50% transparency) at Ares-Vallis showing good visual DTM completeness and co-registration accuracy spatially and vertically compared to the HRSC product. Two profile lines (A & B) are labelled on the map.

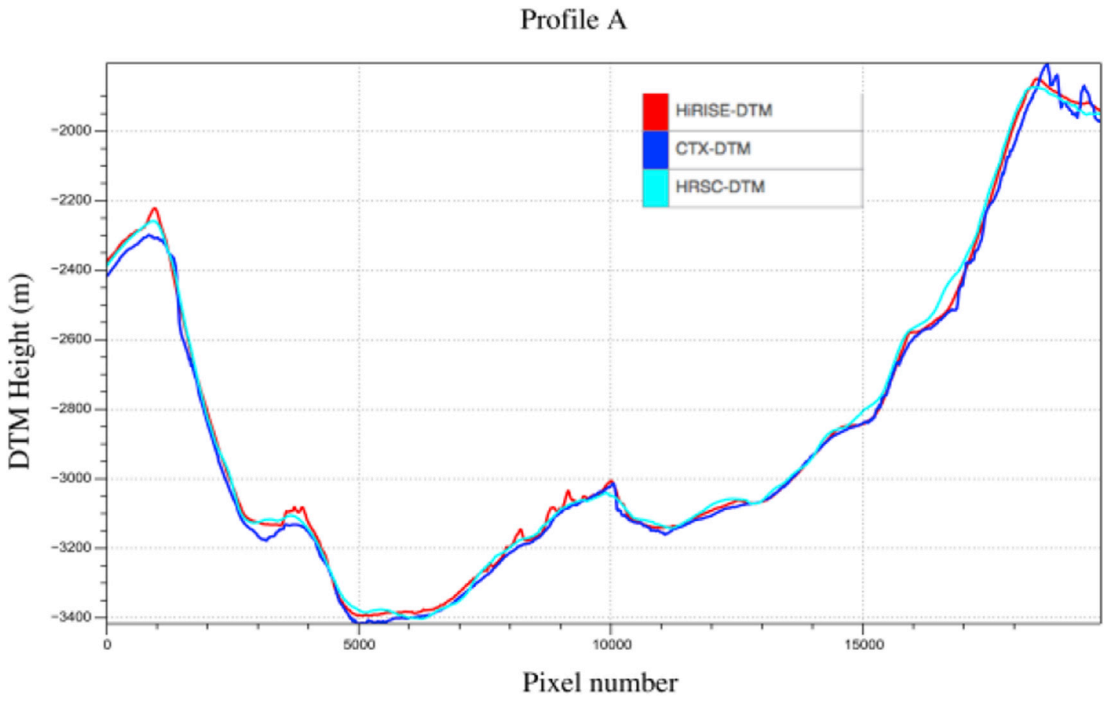

Fig. 27. Profile A for the cascaded HiRISE-CTX-HRSC DTMs at Ares-Vallis.

and 450 metres can be recognized in the CASP-GO MSL CTX DTM with a confidence of 50%. The same is basically true for the UoS DTM though in the next higher crater diameter class the confidence decreases for the UoS data falls to a confidence level of 30%. Hence, only detections of craters with diameters larger than 500 metres can be trusted in the UoS DTM. Hence, we can expect a factor of 1.2× more effective resolution between CASP-GO and the UoS DTM pipeline in the case of the MSL CTX DTM.

From the internal evaluation performed by UCL and an independent evaluation performed by DLR within the iMars project, the resulting CASP-GO DTMs have shown high spatial co-registration accuracy (sub-pixel level) with respect to HRSC (and MOLA) data, improved DTM completeness for unmatched areas, improved DTM accuracy for mismatched areas, and reduced DTM artefacts compared to other DTM routines listed in section 2. CASP-GO was therefore selected for the iMars DTM batch processing software for Mars global CTX and HiRISE DTM production.

4.2. CASP-GO DTMs over MC11-E and MC11-W

During the development of the batch DTM production, CASP-GO was applied to all the CTX images which lay within a large mosaic of HRSC over the U.S. Geological Survey's MC11-E/-W (Fig. 24). For MC11-E, 78 identified stereo pairs were processed. 22 (out of 78) stereo pairs were re-processed with different processing parameters to produce DTMs with

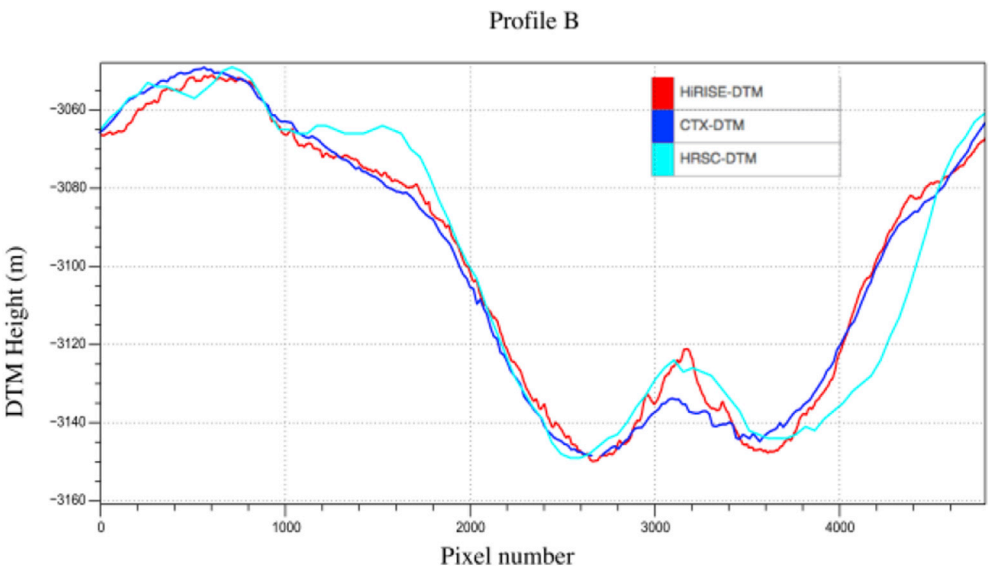

Fig. 28. Profile B for the cascaded HiRISE-CTX-HRSC DTMs at Ares-Vallis.

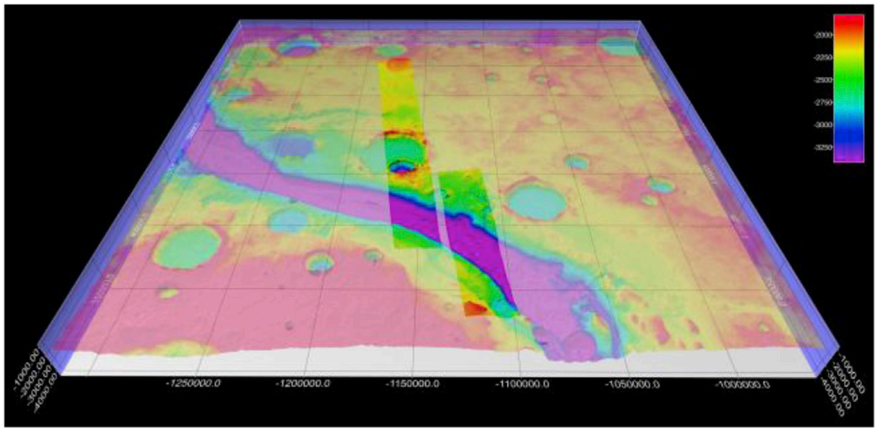

Fig. 29. Fledermaus® view of the processed 18m CTX and 75cm HiRISE DTMs on top of the 50m HRSC MC11-E DTM mosaic at Ares-Vallis. The size of each grid in metres is shown in the above 3D perspective view generated from Fledermaus®.

higher quality. 6 (out of 78, ≈8%) stereo pairs failed and were removed from the processing list because of poor quality associated with one or both of the input images (Fig. 25). 42 (out of 78) non-repeat stereo pairs were integrated to the iMars web-GIS website developed by FUB. Processing of CTX ORI and DTMs over the MC11-E area took ~1.5 weeks' time on 10 Linux processing blades at UCL-MSSL excluding follow-on reprocessing and metadata format changes needed for web-GIS integration. In late 2016, 39 CTX DTM/ORIs over MC11-W were processed using the latest version of the CASP-GO pipeline. These are shown together with the MC11E + W DTM mosaics in (Fig. 24].

The MC11 CTX DTMs are in an equirectangular projection system consistent with the HRSC MC11-E/-W mosaic. They have been shown to have very high spatial and vertical co-registration accuracy compared to the corresponding HRSC DTM mosaic. A subset (Table 7) of the cascaded HiRISE-CTX-HRSC DTMs at Ares-Vallis (Fig. 26) have been used for geologic analysis by geologists at Imperial College London during the iMars public event (http://www.i-mars.eu/outreach/event last accessed: 15.11.2017), demonstrating good DTM quality and high co-registration accuracy. Example profile lines have been extracted from the cascaded HiRISE-CTX-HRSC DTMs which are shown in (Fig. 27 and Fig. 28).

The CASP-GO DTMs show overall good quality in terms of DTM completeness, effective resolution, and co-registration accuracy for the MC11-E/-W area. In the case of Ares-Vallis, the maximum/average differences between CTX and HRSC for Profiles A and B are 98m/14.5m and 30m/12m respectively. Whereas the maximum/average differences between HiRISE and CTX for Profile A and B are 90.5m/11m and 8.5m/3.5m, respectively. The maximum difference is partially subject to large spatial resolution differences between HiRISE, CTX and HRSC.

The co-registered multi-resolution MC11 HiRISE-CTX-HRSC DTM dataset is a valuable resource for geological analysis of the Martian surface for Arabia Terra, Meridiani Planum and Chryse Planitia areas. A 4D geo-spatial processing and analysis tool, called Fledermaus® is used to visualise and perform geological interpretations for the iMars DTM products in subsequent figures.

In Fledermaus, DTMs can be imported as Grid data in several different formats, including Arcview Binary Grid, ASCII Gridded Data, and DTED Grid. For this purpose, GDAL is used to change the file format of the original DTMs from GeoTiff to Binary Gridded Data. Examples of the Fledermaus visualisation of the CASP-GO processed CTX and HiRISE DTMs at Ares-Vallis that are co-registered to the DLR HRSC MC11-E DTM mosaic are shown in (Fig. 29 and Fig. 30).

The 3D scene can be viewed at different angles, transparent scales and vertical exaggerations in Fledermaus®. Profiles along a selected transect can be drawn by “right click and drag”. ORIs can be also draped onto the DTMs in Fledermaus.

4.3. Planet-wide DTM production using CASP-GO

At UCL-MSSL, the ESA HRSC PSA and NASA CTX, HiRISE PDS data volumes have been mirrored in a local shared storage system in order to

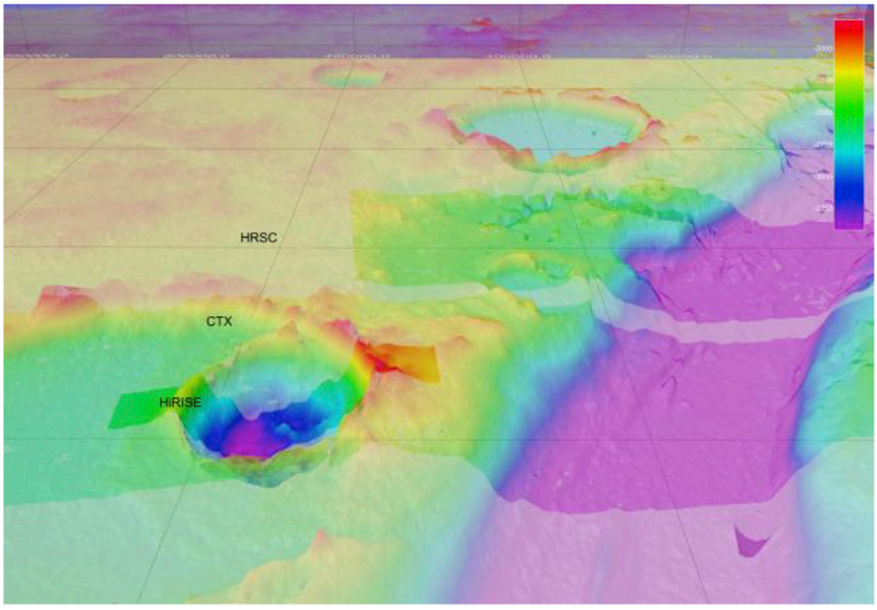

Fig. 30. A zoom-in view of the processed 18m CTX and 75cm HiRISE DTMs on top of the 50m HRSC MC11-E DTM mosaic at Ares-Vallis showing in Fledermaus®.

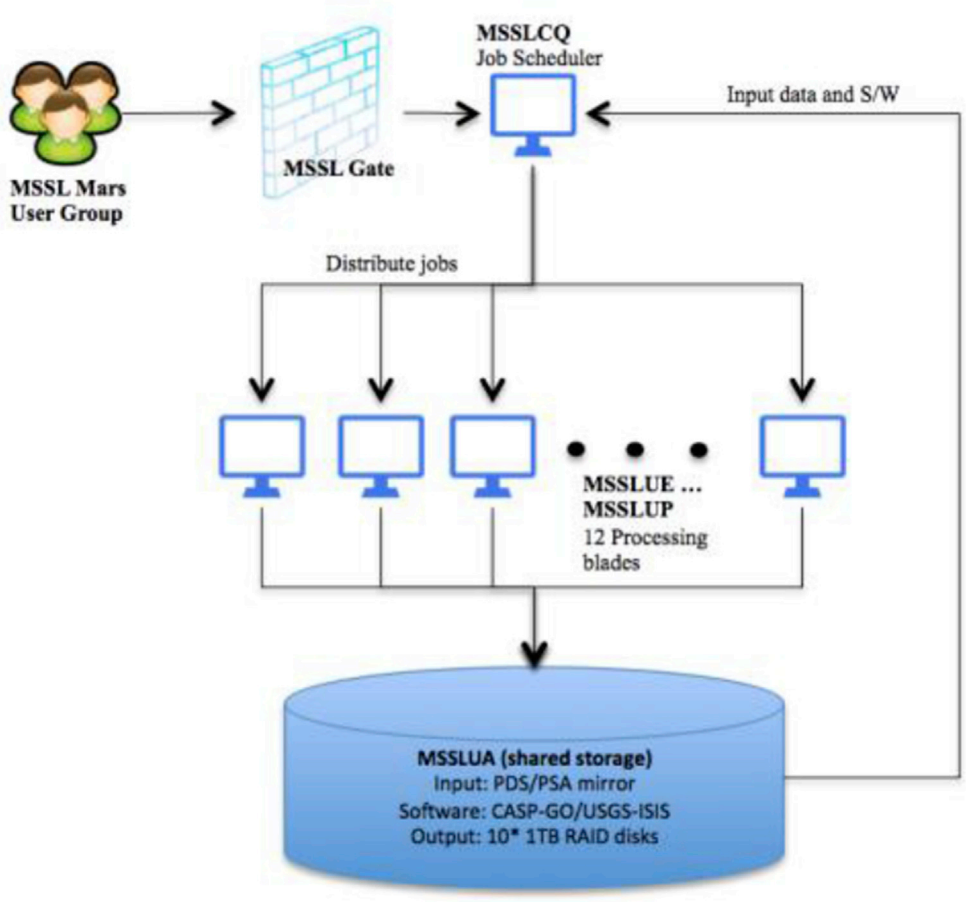

Fig. 31. CASP-GO processing set-up at UCL-MSSL's imaging cluster.

speed up the production process with an option such that if data is unreadable it can be re-read from the original source at the Planetary Science Archives at European Space Astronomy Centre (ESAC) or the NASA PDS at JPL. The software is installed in a shared directory, which is accessible from 14 Linux processing blades (10 with 16 cores and 48GB RAM; 4 with 24 cores and 96GB RAM). Jobs are controlled via a local desktop machine and distributed to the 14 processing blades with multiple sessions of multi-threaded processing. Processed results are stored in RAID storage disk partitions and logged back to the local controlling desktop. Failed jobs can be examined through detailed log files and in the future, could be reprocessed automatically with different processing parameters. A schematic diagram of the UCL-MSSL in-house DTM

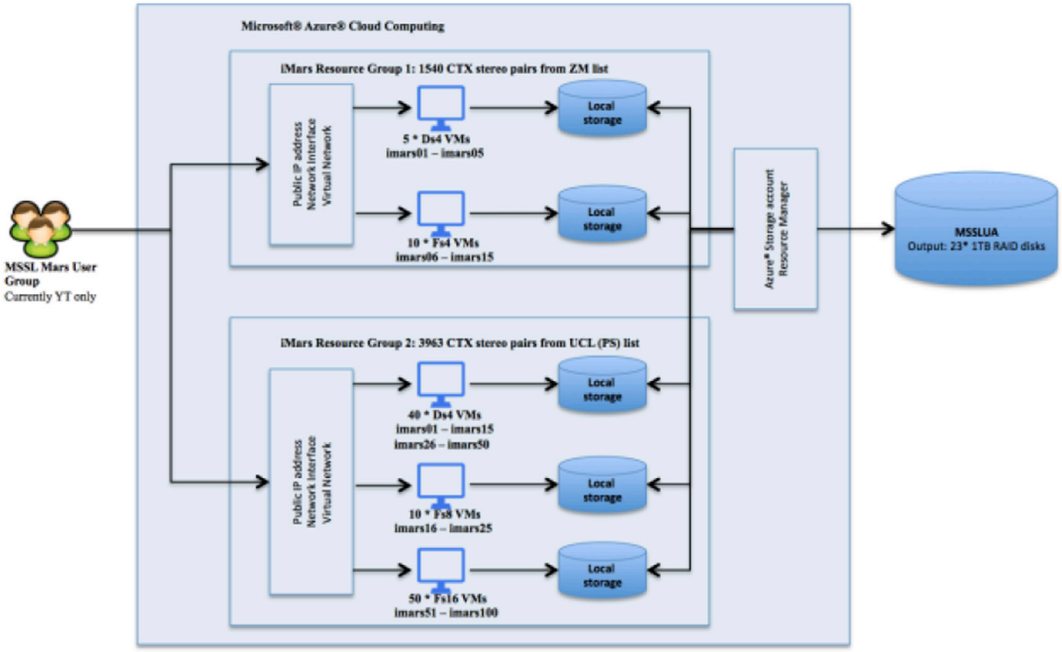

Fig. 32. CASP-GO processing set-up on the Microsoft® Azure® cloud computing resources.

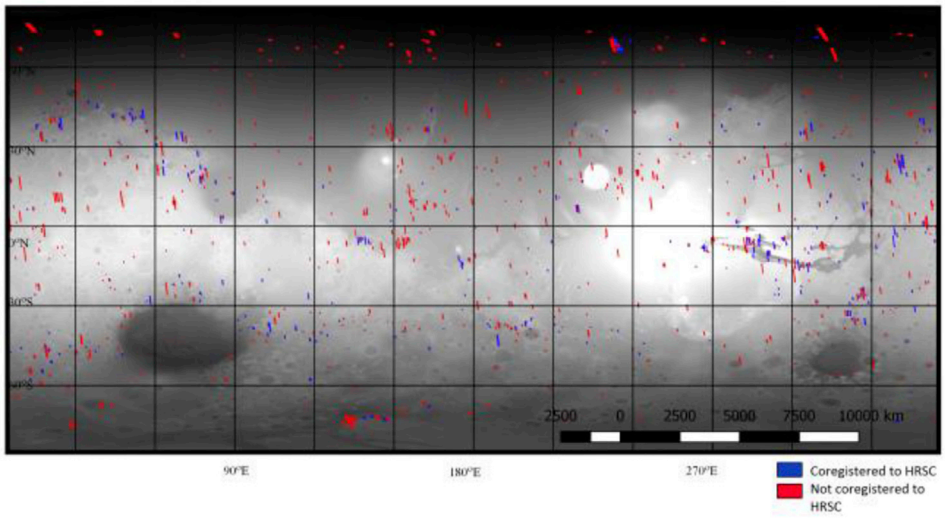

Fig. 33. Location of 1540 18m CTX DTMs processed by the end of 2016. Where no level-4 HRSC DTM exists, the CTX products are not co-registered to a global co-ordinate system. These are shown in red. (For interpretation of the references to colour in this figure legend, the reader is referred to the Web version of this article.)

production structure is shown in (Fig. 31). However, with processing pressure from the large number of CTX DTMs and huge image sizes from HiRISE, we decided to use cloud-computing resources for the planet-wide DTM production.

In mid 2016, a total of 1540 CTX stereo pairs with global coverage of Martian surface were started to be processed on the Microsoft® Azure® cloud computing resource for massive scale batch processing. By late February 2017, a further 3963 stereo pairs were selected (Sidiropoulos and Muller, 2015) and set-up for batch processing on a very large number (150) of Virtual Machines (VMs) on the Microsoft® Azure® Cloud computing. A systematic diagram of the CASP-GO processing set-up at Microsoft® Azure® cloud computing VMs is shown in (Fig. 32).

By December 2016, a total of 1540 CTX stereo pairs had been processed to DTMs and ORI using the CASP-GO pipeline. A graphic showing the location of the 1540 CTX DTMs that have been processed is shown in (Fig. 33). The North Pole and South Pole coverage are shown in (Fig. 34 and Fig. 35) respectively. The blue footprints are CTX DTMs that have been co-registered to HRSC DTMs. Where, there is no level-4 HRSC DTM available, the CTX DTMs are not co-registered to HRSC and these are shown as red footprints. The 1540 CTX DTMs cover 8.76% (12,691,808.505 km^2) of the whole Martian surface (144.8 million km^2). Within this, 4.16% (6,028,461.237 km^2) is covered with co-registered CTX DTMs, the remaining 4.6% (6,663,347.268 km^2) don't have level-4 HRSC DTM available, and hence are not co-registered to the global co-ordinate system.

In early 2017, 3963 further CTX stereo pairs were ingested into the Microsoft® Azure® cloud computing system. By July 2017 3963 CTX DTMs had been processed. A graphical plot of the 3963 CTX DTMs that have been processed is given in (Fig. 36). The equivalent North and South Polar coverage are shown in (Fig. 37 and Fig. 38). The 3963 CTX DTMs cover a further 19.45% (28,158,162.125 km^2) of the whole Martian surface (144.8 million km^2). Within this, 8.54% (12,366,747.357 km^2) are covered with co-registered CTX DTMs, with the remaining 10.91% (15,791,414.76 km^2) not having level-4 HRSC DTMs yet available. The overall statistics for CTX are 1915 pairs have HRSC out of the total. Out of 1540,882 pairs don't have HRSC coverage. Out of 3963, 2491 pairs don't

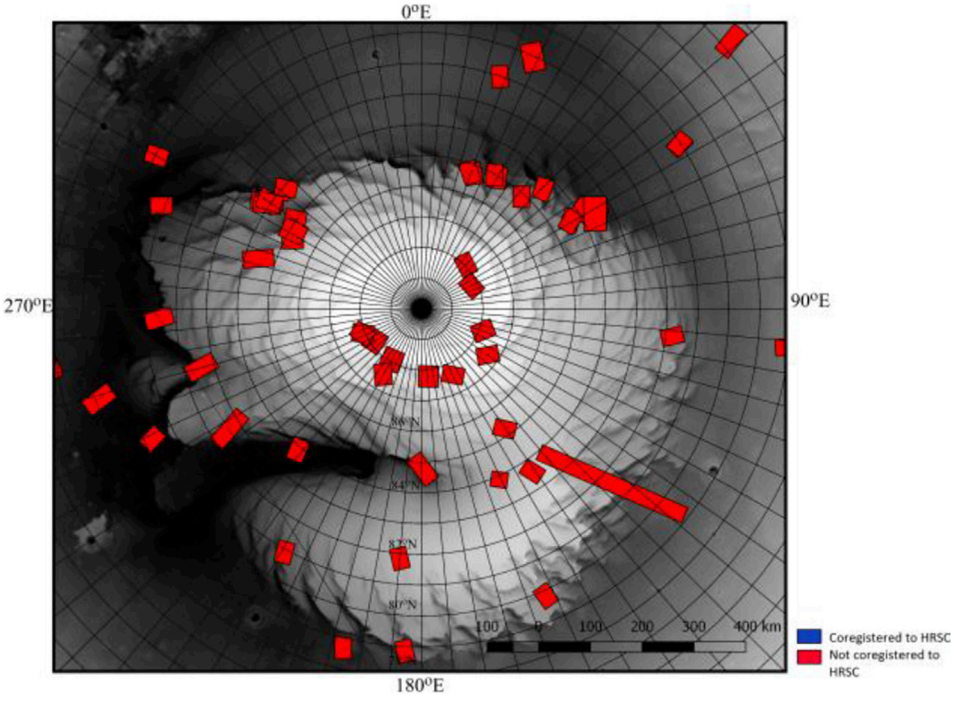

Fig. 34. North Polar coverage of CTX DTMs (116) in the processed 1540-set.

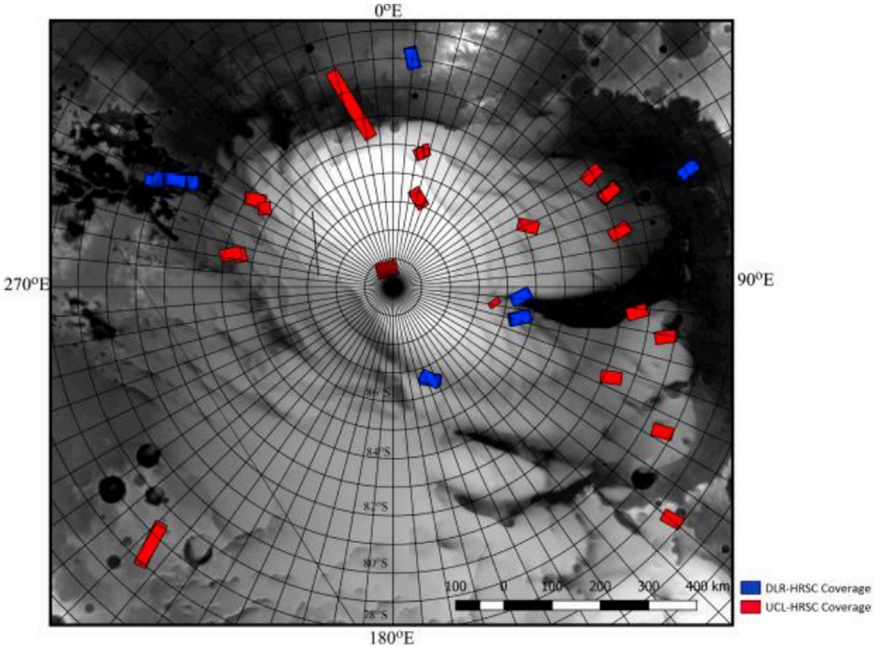

Fig. 35. South Polar coverage of CTX DTMs (106) in the processed 1540-set.

have HRSC. However, for the polar regions, there is now a complete set of level-4 data prior to writing up this paper, so CTX DTMs in (Fig. 35 and Fig. 38) will be updated in the future with respect to HRSC co-registration. All the 1540 DTMs (≈900) have been visually inspected with respect to quality. Less than 5% had unacceptable quality due to either one or both input images having poor quality (see below for further details).

Meanwhile, a number of HiRISE DTMs are being processed in the AWS® cloud computing VMs out of the total of 441 stereo pairs for the areas that have 5 or more repeat HiRISE observations that are scientifically interested for surface change detection and super-resolution restoration. This processing is still on-going at the time of writing. Once as many of the HiRISE stereo-pairs as can be completed within the AWS® resources available, they will be integrated with the existing UoA processed HiRISE DTMs within the iMars webGIS. The global coverage of the UCL HiRISE DTMs that are being processed and the UoA processed HiRISE DTMs are shown in (Fig. 39). The North and South Polar coverage are shown in (Fig. 40 and Fig. 41).

The UoA and USGS processed HiRISE DTMs (with a total number of 468 to date) currently cover 0.183% (210,513.716 km^2) of the Martian surface. The UCL 441 HiRISE DTMs that are being processed for potential change detection (repeat) sites only have one overlap with the UoA PDS processed HiRISE DTMs. The UCL HiRISE DTMs will hopefully cover 0.168% (192,721.942 km^2) of the Martian surface. Once all of the HiRISE

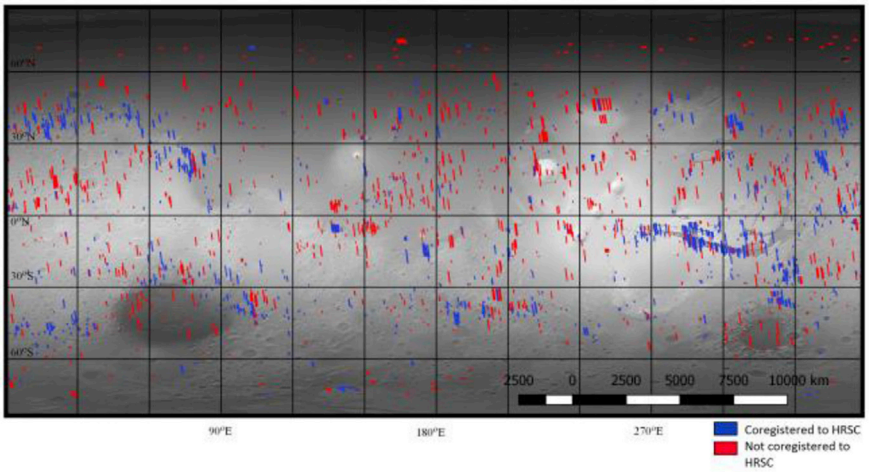

Fig. 36. Locations of all the 3963 CTX stereo-pairs processed on Microsoft Azure® including overlaps.

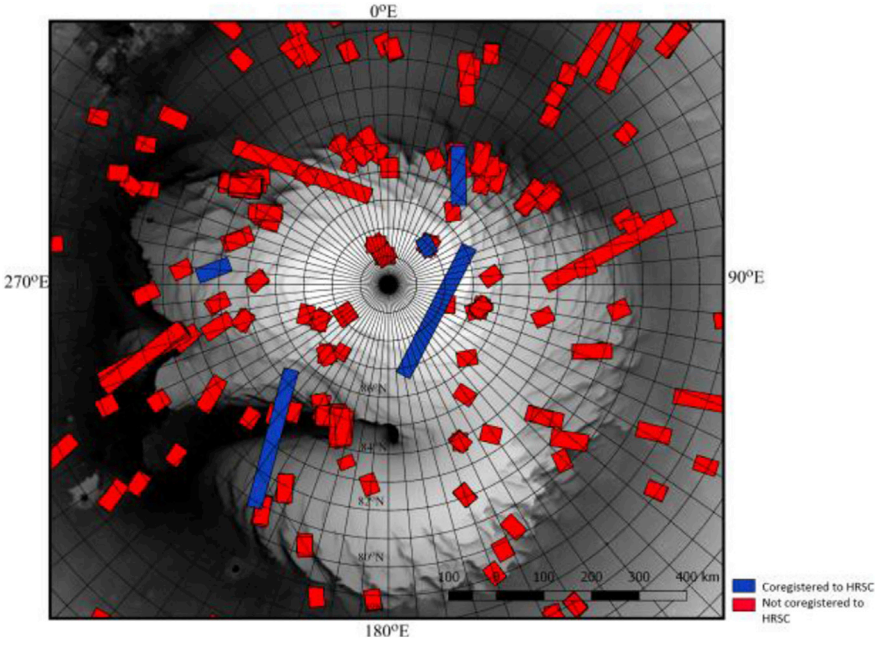

Fig. 37. North Polar coverage of CTX DTMs (591) in the processed 3963-set.

DTMs are complete, they will be integrated into the iMars webGIS system by UCL and be available to the planetary science community. Note that the UoA DTMs are originally not co-registered to HRSC. Once the 3963 CTX DTMs and ORIs are finished, the UoA HiRISE DTMs and ORIs will be co-registered to the CTX products available. An example of the co-registered UCL CASP-GO CTX DTM and separately co-registered UoA HiRISE DTM at the South Pole region is given in (Fig. 42). The cascaded HiRISE-CTX-HRSC dataset shows good spatial and vertical consistency to each other within the Fledermaus® 3D visualisation software (Fig. 43) for geological analysis.

4.4. Visual inspection and evaluation

In iMars, a quantitative evaluation and validation process has been performed based on the experimental ORIs and DTMs as discussed in section 4.1 and section 4.2. Besides, a large number of the batch processed DTMs in section 4.3 have been assessed using a 5-star rating scheme, i.e. 1 – failed, 2 – major problem, 3 – minor problem, 4 – good quality, 5 – excellent quality. 503 out of 620 DTMs have been rated as 3+, i.e. 316 good and excellent, 187 with minor problem. 31 out of 620 failed all due to bad input images (5%) demonstrated previously, which are impossible for DTM processing. Some examples of the visual inspections are given in (Fig. 44). (Fig. 44 (A)) shows DTMs with minor problem, for example, A-1 has small gaps inside the crater, A-2 has minor jitter problems and minor gaps around the crater edge, A-3 has a small gap around crater edge. For more examples, please visit the iMars webGIS (http://www.i-mars.eu/web-gis last accessed: 15.11.2017).

5. Discussion

The CASP-GO pipeline has been demonstrated to produce improved results when compared with the original ASP pipeline in a fully automated manner. However, there are known issues including:

a) Lack of a de-jittering procedure. From the visual inspection of the HiRISE DTM products, we noticed some of them have jitter issues which cannot be fixed using existing de-jittering software. For example, the USGS-ISIS hijitter function currently cannot remove the jitter effect in most cases. We have used dejittered HiRISE images from the UoA dejitter team to cope with this issue.

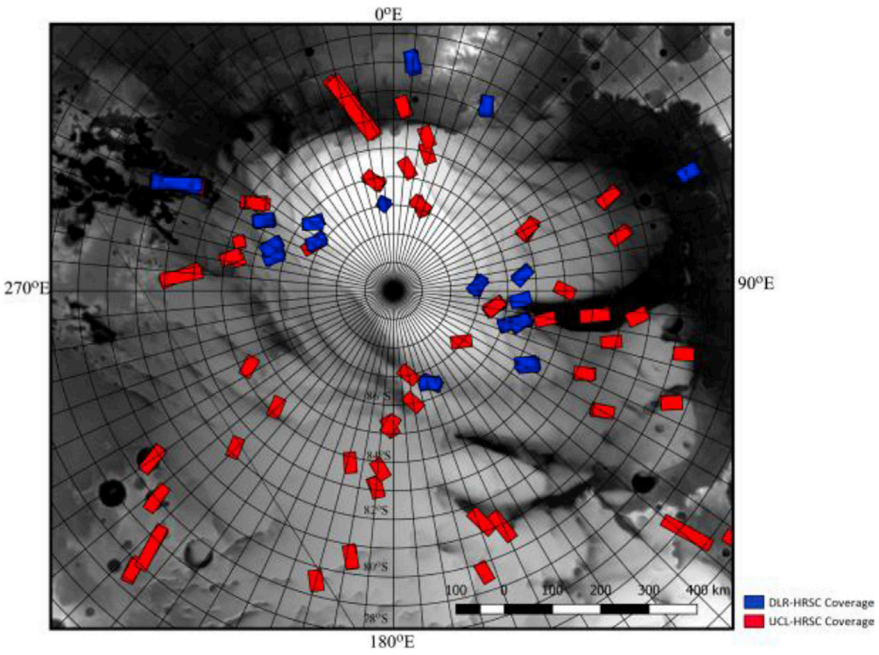

Fig. 38. South Polar coverage of CTX DTMs (287) in the processed 3963-set.

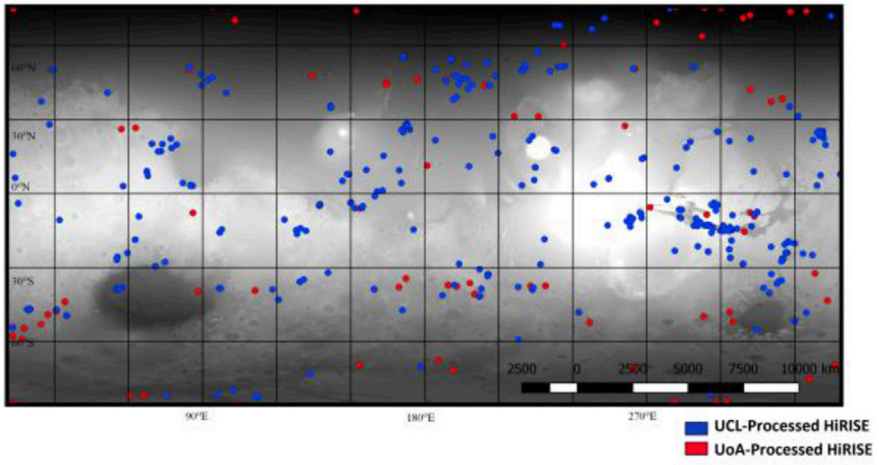

Fig. 39. Global coverage of UCL HiRISE DTMs and UoA HiRISE DTMs in Equirectangular projection system. Footprint sizes highly exaggerated to make them visible.

b) Lack of a radiometric de-calibration procedure. We also observed striping artefacts from some of the CTX DTM products that appear to be related to poor radiometric de-calibration from the USGS-ISIS functions when converting raw PDS files to the USGS-ISIS cub files. We are currently working on a posteriori pattern filtering post-processing system to eliminate these striping artefacts.
c) No options for an adaptive kernel size. The ASP matching kernel size and Gotcha kernel size are all set in the input parameter files. Users can change it every time they use CASP-GO. However, for batch processing, the larger matching kernel size may result in smoother results for feature rich areas, although this is currently necessary for batch processing to reduce mis-matches. Currently, CASP-GO can't select the optimum kernel size automatically for each stereo pair for large-scale batch processing. We plan to investigate different strategies in future to deal with these issues.
d) Quilting artefacts from the ASP cross-correlation cannot be completely removed at this time. Although we are able to remove the quilting artefact from flat areas, there is still a chance that it can occur on steep slopes. We are hoping that the pattern filtering post-process will eliminate this artefact as well.
e) There is currently no effective point cloud co-registration procedure in CASP-GO (other than the BA function provided by the USGS-ISIS and ASP) to perform accurate vertical co-registration. In comparison to HRSC, CTX shows large vertical differences at the image borders for large area DTMs.
f) The computation time of CASP-GO is pretty high. We have to trade-off some quality and accuracy by reducing the kernel size and number of iterations of the ALSC process for HiRISE and especially for the planet-wide big data processing. We hope the CASP-GO components will be further improved by the NASA Ames team and the planetary mapping community through the release of open source components.

6. Data downloads and visualisation

6.1. PDS labelling

In order to permit subsequent release of iMars data products through

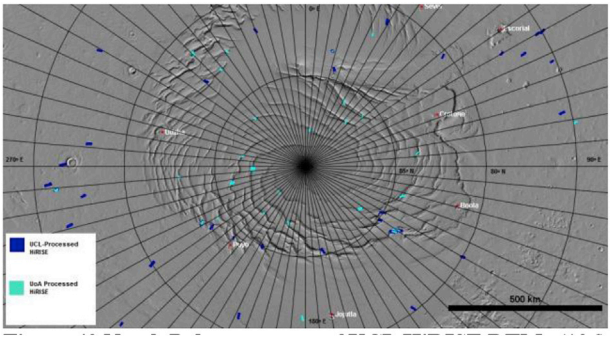

Fig. 40. North Polar coverage of UCL HiRISE DTMs (106) and UoA HiRISE DTMs (27) in the processed 441-set.

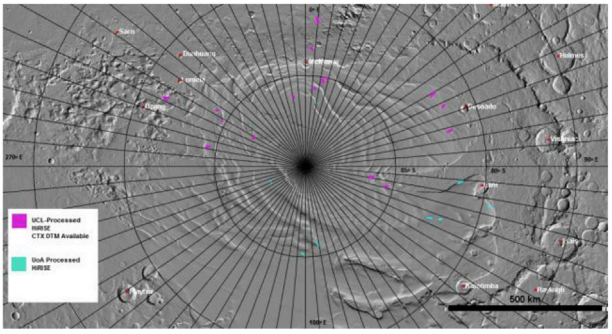

Fig. 41. South Pole coverage of UCL HiRISE DTMs (43) and UoA HiRISE DTMs (12) in the processed 441-set.

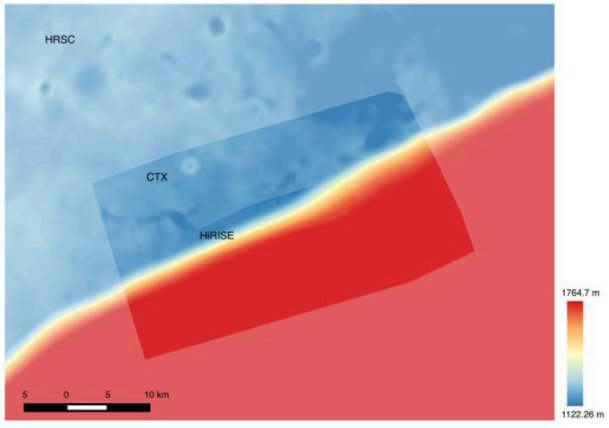

Fig. 42. CASP-GO CTX DTM (70% transparency) and co-registered UoA HiRISE DTM (100% transparency) showing on top of the UCL HRSC DTM (50% transparency) at SPRC.

PDS and PSA, we have followed the label naming conventions and type specifications designed for PDS3. The CASP-GO DTM processing chain used the Parameter Value Language (PVL), which is a markup language commonly employed for entries in the PDS, to store metadata. A Python implementation of PVL can be found from (https://github.com/planetarypy/pvl last accessed: 15.11.2017) for encoding and decoding a superset of PVL, including the USGS-ISIS Cube Label and NASA PDS3 Label dialects.

The output PVL format metadata from CASP-GO contains: a) processing information including processing software versions, operating system, resource, start and end time; b) metadata information includes image ID, format, bit depth, resolution, nodata value, and map projections; c) algorithm information includes ASP parameters, sGotcha parameters, f-ML parameters, ORS parameters, co-kriging parameters, and MSA-SIFT parameters.

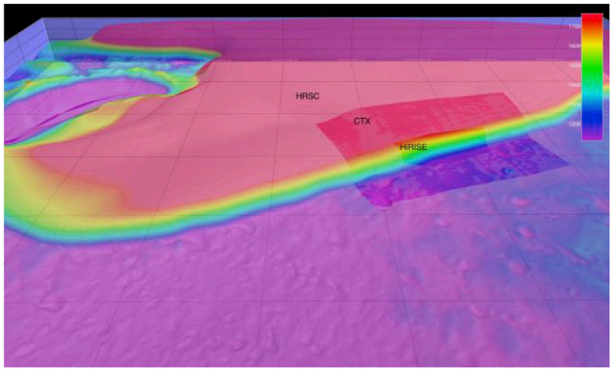

Fig. 43. 3D visualisation of the co-registered UoA HiRISE, UCL CTX, and UCL HRSC DTMs at SPRC. The unit of the grids is in metres.

The Advanced Multi-Mission Operations System (AMMOS) PDS Pipeline Service (APPS) is an end-to-end pipeline for PDS archiving, which streamlines the delivery of science data to the PDS. In collaboration with the APPS team at JPL, it was demonstrated that the PVL metadata used in CASP-GO is compatible and fully convertible to the PDS4 label by using the online label design tool (https://apps-ldt.jpl.nasa.gov/ last accessed: 15.11.2017) and label validation tool (https://pds.nasa.gov/pds4/software/validate/last accessed: 15.11.2017).

We are working with the APPS-PDS4 team and would like to publish the highest quality processed global CTX and HiRISE DTMs via PDS4 in the near future. In the interim, any scientists interested in these products should contact the iMars co-ordinator (second author).

6.2. iMars Web-GIS

In iMars, an interactive web-mapping platform was developed for the purpose of visualising and downloading the products created by the project (Walter et al., 2017) which has recently been ported to the UCL-MSSL imaging server (http://www.i-mars.eu/web-gis last accessed: 15.11.2017) in collaboration with FUB. The web-GIS builds exclusively upon open-source technology and Open Geospatial Consortium (OGC)/International Organisation for Standardisation (ISO) standards to allow for a high level of interoperability and scalability. It includes a server backend together with file storage, a browser-based front-end and a spatial database management system. The web-GIS is capable of interactively display the described DTM and image products in an intuitive user interface consisting of a familiar map environment. It is adapted to deliver a large amount of available data products very efficiently to allow smooth panning and zooming of the high detailed data products to enable the user to perform interactive inspection of the data. The basis of the web-based map display is a web map service (WMS) protocols with customised coordinate reference systems suitable for Mars projections (equidistant cylindrical and polar stereographic, respectively).

In the iMars web-GIS, the CASP-GO terrain models are categorised as dedicated layers in the group “CTX/HiRISE Digital Terrain Models” with individual layers for the particular instruments. The data are shown as hill-shaded reliefs encoded with a planet-wide global pseudo colour table. The models seamlessly integrate with the other topographic products available in the web-GIS, mainly the HRSC DTMs in their multi-orbit bundle-block-adjusted and single strip bundle-adjusted versions (Gwinner et al., 2016). All DTM layers are visualised with the same hill-shading parameters and colour ramp, which enables a consistent user experience while smoothly zooming through the various datasets with their different levels of resolution and detail.

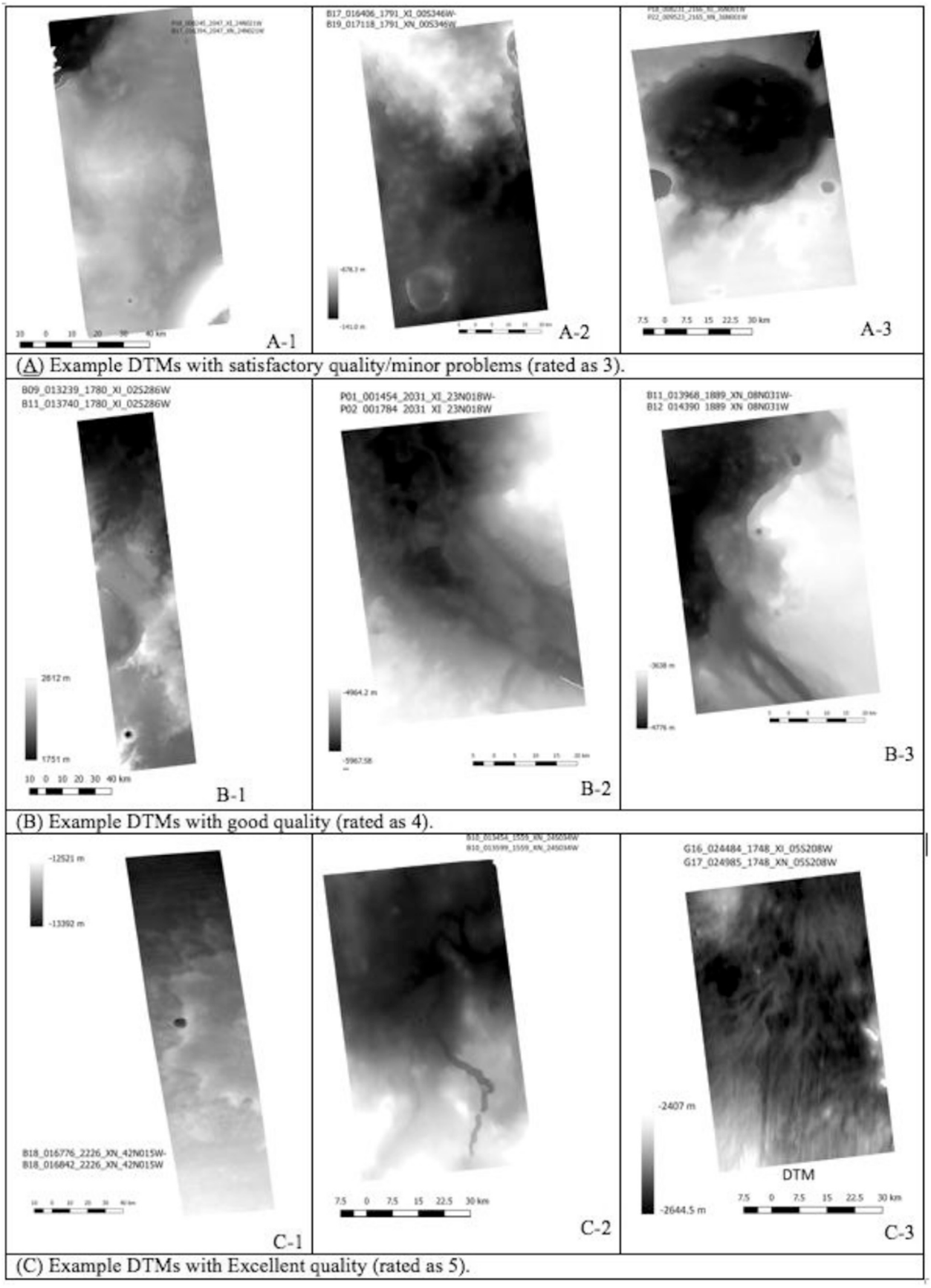

Fig. 44. Examples of rated CTX DTMs after visual inspection.

Besides the DTMs, the co-registered ortho-rectified images (ORI) resulting from the CASP-GO pipeline are available as separate layers in the group "CTX/HiRISE OrthoRectified Images". The panchromatic images have been converted to 8-bit format beforehand. For performance considerations, all data have been re-projected to either the equidistant cylindrical projection for the equatorial view or to the polar stereographic projections for the polar views (>75°) with the changeover occurring between 45 and 60° of latitude. The topographic DTM layers act as base layers in the web-GIS – further data layers consist of the HRSC multi-orbit image mosaics in grayscale and colour, a global high-resolution repeat coverage map in colour and vector maps for nomenclature and landing sites markers. Footprints for the main NASA mission's instruments available from the PDS Mars Orbital Data Explorer (ODE) are also included with time support – a dedicated time slider lets the user filter for particular start and stop times in either Martian or Earth time.

The iMars web-GIS contains extended functionalities for the HRSC single images and the ACRO images from within iMars, bundled in a dedicated toolbar for the visualisation of these time-series of single images (HRSC and other datasets registered to HRSC). The footprint layers can be queried for the metadata attributes hosted in a spatial database. The metadata is derived from regular processing using ISIS as well as from the additional processing tasks performed during the DTM and ORI generation.

We plan to extend the attribute query capabilities and also link against the actual data product downloads once they are available in the PDS archive.

To handle the large datasets and provide an efficient user interface, all the WMS data are streamed to the client as tiles. The tiles are automatically cached in the browser. On the server side, a tile cache has been implemented to allow pre-calculating the tiles for different zoom levels. This way the system speed is highly optimised – internal tests have demonstrated that the system is capable of serving ten concurrent users with highly demanding tasks.

7. Summary and future work

Within the recently completed EU FP-7 iMars project, we tested/evaluated several popular planetary DTM pipelines including two in-house DTM pipelines from iMars partners, in which the NASA ASP software showed the best performance against the others. Then we introduced the proposed CASP-GO DTM processing chain, based on the open source ASP software, tie-point based multi-resolution image co-registration, Gotcha sub-pixel refinement, and co-kriging method.

We demonstrated that the CASP-GO pipeline appears to produce the best results in terms of improved global geo-referencing with respect to HRSC (and thence to MOLA), and refined stereo matching completeness and accuracy from the ASP normalised cross-correlation using CTX and HiRISE test data at the MER and MSL rover sites. We addressed issues and artefacts discovered from experimenting with the ASP software, especially on dealing with failed matching, mis-matches, and quality-efficiency trade-offs.

We then introduced the batch DTM processing system at the MSSL imaging cluster for the USGS MC11 area, showing co-registered multi-resolution DTMs from HiRISE, CTX and HRSC, and provided examples of evaluation of the cascaded datasets. A more up to date, global, non-repeat CTX stereo list and repeat-pass HiRISE stereo list was introduced. These CTX and HiRISE stereo pairs are being processed using the CASP-GO pipeline at Microsoft® Azure® and Amazon® AWS cloud computing resources. The global footprint map and an initial qualitative evaluation of the ~4000 CTX DTMs is provided.

All sufficiently high-level quality products and all software shown in this work are planned to be made open-source to the planetary science community. The CASP-GO pipeline is planned to be made open-source through the NASA Ames Github. The processed ORIs and DTMs will eventually be publicly available through the NASA PDS via the APPS-PDS4 collaboration. The derived products including colourised hillshaded DTMs, footprints, and other GIS and map products are already available through the iMars web-GIS system.

In the future, the processed multi-resolution co-registered DTM products can be applied to assist the ESA ExoMars 2020 rover mission and the CASP-GO software will be applied to the ESA ExoMars Trace Gas Orbiter 2016 CaSSiS instrument to provide high-quality co-registered colour stereo.

Acknowledgements

The research leading to these results has received funding from the European Union's Seventh Framework Programme (FP7/2007-2013) under iMars grant agreement n° 607379 as well as partial funding from the STFC "MSSL Consolidated Grant" ST/K000977/1. The authors would like to thank J.R. Kim for use of the UoS DTM results, and A. Ivanov for the CTX DTMs employed for the assessments shown in section 2 as well as K. Willner for use of some of his validation results and Mike Lusty, Akira and Kira Koch for volunteering their time for the visual CTX DTM quality assessment.

References

Becker, K.J., et al., 2013. ISIS support for NASA mission instrument ground data processing systems. Lunar Planet. Sci 44. XLIV, Houston, Texas, Abstract #2829.

Beyer, R.A., 2015. An introduction to the data and tools of planetary geomorphology. Geomorphology 240, 137–145.

Cook, A.C., Oberst, J., Roatsch, T., Jaumann, R., Acton, C., 1996. Clementine imagery: selenographic coverage for cartographic and scientific use. Planet. Space Sci. 44, 1135.

Day, T., Muller, J., 1989. Digital elevation model production by stereo-matching SPOT image-pairs - a comparison of algorithms. Image Vis Comput. 7 (2), 95–101.

Edwards, K., 1987. Geometric processing of digital images of the planets. Photogramm. Eng. Rem. Sens. 53 (9), 1219–1222.

Griin, A., 1985. Adaptive least squares correlation: a powerful image matching technique. South African Journal of Photogmmmetry. Remote Sensing and Cartography 14 (3), 175–187.

Gupta, R., Hartley, R., 1997. Linear pushbroom cameras. IEEE Trans. Pattern Anal. Mach. Intell. 19 (9), 963–975.

Gwinner, K., Scholten, F., Spiegel, M., Schmidt, R., Giese, B., Oberst, J., Jaumann, R., Neukum, G., 2009. Derivation and validation of high-resolution digital terrain models from mars express HRSC data. Photogramm Eng Rem S 75 (9), 1127–1142.

Gwinner, K., Jaumann, R., Bostelmann, J., Dumke, A., Elgner, S., Heipke, C., Kersten, E., Michael, G., Preusker, F., Roatsch, T., Schmidt, R., 2015. The First Quadrangle of the Mars Express HRSC Multi Orbit Data Products (MC-11-e).

Gwinner, K., Jaumann, R., Hauber, E., Hoffmann, H., Heipke, C., Oberst, J., Neukum, G., Ansan, V., Bostelmann, J., Dumke, A., Elgner, S., Erkeling, G., Fueten, F., Hiesinger, H., Hoekzema, N.M., Kersten, E., Loizeau, D., Matz, K.-D., McGuire, P.C., Mertens, V., Michael, G., Pasewaldt, A., Pinet, P., Preusker, F., Reiss, D., Roatsch, T., Schmidt, R., Scholten, F., Spiegel, M., Stesky, R., Tirsch, D., van Gasselt, S., Walter, S., Wahlisch, M., Willner, K., 2016. The high resolution stereo camera (HRSC) of mars express and its approach to science analysis and mapping for mars and its satellites. Planet. Space Sci. 126, 93–138.

Heipke, C., Oberst, J., Albertz, J., Attwenger, M., Dorninger, P., Dorrer, E., Ewe, M., Gehrke, S., Gwinner, K., Hirschmüller, H., Kim, J.R., 2007. Evaluating planetary digital terrain models—the HRSC DTM test. Planet. Space Sci. 55 (14), 2173–2191.

Ivanov, A.B., 2003. Ten-meter scale topography and roughness of mars exploration rovers landing sites and martian polar regions. In: 34th Annual Lunar and Planetary Science Conference. League City, Texas, abstract no. 2084.

Ivanov, A.B., Lorre, J.J., 2002. Analysis of mars orbiter camera stereo pairs. In: 33rd Annual Lunar and Planetary Science Conference. Houston, Texas, abstract no.1845.

Kim, J., Muller, J.-P., 2009. Multi-resolution topographic data extraction from Martian stereo imagery. Planet. Space Sci. 57, 2095–2112.

Kirk, R.L., Howington-Kraus, E., Rosiek, M.R., Anderson, J.A., Archinal, B.A., Becker, K.J., Cook, D.A., Galuszka, D.M., Geissler, P.E., Hare, T.M., Holmberg, I.M., Keszthelyi, L.P., Redding, B.L., Delamere, W.A., Gallagher, D., Chapel, J.D., Eliason, E.M., King, R., McEwen, A.S., HiRISE Team, 2008. Ultrahigh resolution topographic mapping of Mars with MRO HiRISE stereo Images: meter-scale slopes of candidate Phoenix landing sites. J. Geophys. Res. 113 https://doi.org/10.1029/2007JE003000. E00A24.

Li, R., Hwangbo, J.W., Chen, Y., Di, K., 2008. Rigorous photogrammetric processing of HiRISE stereo images for topographic mapping, International Archives of the Photogrammetry. Remote Sensing and Spatial Information Sciences 37 (B4), 987–992.

Lowe, D., 2004. Distinctive image features from scale-invariant keypoints. Int. J. Comput. Vis. 60 (2), 91–110.

McEwen, A.S., et al., 2007. Mars reconnaissance Orbiter's high resolution imaging science experiment (HiRISE). J. Geophys. Res. 112 https://doi.org/10.1029/2005JE002605. E05S02.

Moratto, Z.M., Broxton, M.J., Beyer, R.A., Lundy, M., Husmann, K., 2010. Ames stereo pipeline, NASA's open source automated stereogrammetry software. Lunar and Planetary Science Conference 41 abstract #2364.

Olson, C., Maximum-Likelihood Image Matching, 2002. In: IEEE Transactions on Pattern Analysis and Machine Intelligence, vol. 24, 6.

Paar, G., Waugh, L., Barnes, D., Pajdla, T., Woods, M., Graf, H.-R., Gao, Y., Willner, K., Muller, J.-P., Li, R., 2012. Integrated field testing of planetary robotics vision processing: the PRoVisG campaign in Tenerife 2011. Prof. SPIE on Intelligent Robots and Computer Vision XXIX: Algorithms and Techniques 8301, 83010O–1–18.

Shean, D.E., Alexandrov, O., Moratto, Z., Smith, B.E., Joughin, I.R., Porter, C.C., Morin, P.J., 2016. An automated, open-source pipeline for mass production of digital elevation models (DEMs) from very high-resolution commercial stereo satellite imagery. ISPRS J. Photogrammetry Remote Sens. 116.

Shin, D., Muller, J.-P., 2012. Progressively weighted affine adaptive correlation matching for quasi-dense 3D reconstruction. Pattern Recogn. 45 (10), 3795–3809.

Sidiropoulos, P., Muller, J.-P., 2015. Matching of large images through coupled decomposition. IEEE Trans. Image Processing 24 (7), 2124–2139. https://doi.org/10.1109/TIP.2015.2409978.

Sidiropoulos, P., Muller, J.-P., 2017. A systematic solution to multi-instrument co-registration of high-resolution planetary images to an orthorectified baseline. IEEE Transactions on Geoscience and Remote Sensing. https://doi.org/10.1016/j.pss.2017.10.012.

Smith, D.E., Zuber, M.T., Frey, H.V., Garvin, J.B., Head, J.W., Muhleman, D.O., Pettengill, G.H., Phillips, R.J., Solomon, S.C., Zwally, H.J., Banerdt, W.B., Duxbury, T.C., Golombek, M.P., Lemoine, F.G., Neumann, G.A., Rowlands, D.D., Aharonson, Oded, Ford, P.G., Ivanov, A.B., Johnson, C.L., McGovern, P.J., Abshire, J.B., Afzal, R.S., Sun, Xiaoli, 2001. Mars orbiter laser altimeter—experiment summary after the first year of global mapping of mars. J. Geophys. Res. 106 (E10), 23,689–23,722.

Stein, M.L., 1999. Statistical Interpolation of Spatial Data: Some Theory for Kriging. Springer, New York.

Tao, Y., Muller, J.-.P., 2016. A novel method for surface exploration: super-resolution restoration of Mars repeat-pass orbital imagery. Planet. Space Sci. 121, 103–114.

Tao, Y., Muller, J.-P., Poole, W., 2016. Automated localisation of Mars rovers using co-registered HiRISE-CTX-HRSC orthorectified images and wide baseline Navcam orthorectified mosaics. Icarus 280, 139–157.

Thomas, N., Cremonese, G., Ziethe, R., Gerber, M., Brändli, M., Bruno, G., Erismann, M., Gambicorti, L., Gerber, T., Ghose, K., Gruber, M., Gubler, P., Mischler, H., Jost, J., Piazza, D., Pommerol, A., Rieder, M., Roloff, V., Servonet, A., Trottmann, W., Uthaicharoenpong, T., Zimmermann, C., Vernani, D., Johnson, M., Pelò, E., Weigel, T., Viertl, J., De Roux, N., Lochmatter, P., Sutter, G., Casciello, A., Hausner, T., Veltroni, I.F., Da Deppo, V., Orleanski, P., Nowosielski, W., Zawistowski, T., Szalai, S., Sodor, B., Tulyakov, S., Troznai, G., Banaskiewicz, M., Bridges, J.C., Byrne, S., Debei, S., El-Maarry, M.R., Hauber, E., Hansen, C.J., Ivanov, A., Keszthelyi, L., Kirk, R., Kuzmin, R., Mangold, N., Marinangeli, L., Markiewicz, W.J., Massironi, M., Mcewen, A.S., Okubo, C., Tornabene, L.L., Wajer, P., Wray, J.J., 2017. The colour and stereo surface imaging system (CaSSIS) for the ExoMars Trace Gas orbiter. Space Sci. Rev. 1–48. https://doi.org/10.1007/s11214-017-0421-1.

Traxler, C., Ortner, T., Hesina, G., Barnes, R., Gupta, S., Paar, G., Muller, J.-P., Tao, Y., Willner, K., 2017. The PRoViDE Framework: accurate 3D Geological Models for Virtual Exploration of the Martian Surface From Rover and Orbital Imagery, AGU Book Chapter 3D Digital Geological Models: from Terrestrial Outcrops to Planetary Surfaces (in press).

Veitch-Michaelis, J., 2016. Fusion of LIDAR with Stereo Camera Data - an Assessment (Unpublished UCL PhD Thesis).

Walter, S.H.G., Muller, J.-P., Sidiropoulos, P., Tao, Y., Gwinner, K., Putri, A.R.D., Kim, J.-R., Steikert, R., van Gasselt, S., Michael, G.G., 2017. The iMars web GIS - an interactive online mapping tool for the spatio-temporal visualization of topography data and dynamic time-series of single image layers ISPRS. Journal of Photogrammetry and Remote Sensing submitted for publication.